https://doi.org/10.5194/egusphere-2026-3354
Preprint. Discussion started: 10 July 2026

Multi-year convection-permitting irrigation impacts across the European continent

Jane Leonor Roque[1] and Arianna Valmassoi[2]

[1]Institute of Geosciences, Meteorology Section, University of Bonn, Bonn, Germany
[2]Deutscher Wetterdienst, Offenbach am Main, Germany

Correspondence: Jane Leonor Roque (jroquema@uni-bonn.de)

Abstract. Irrigation representation in weather and climate modeling is advancing and becoming more relevant. Global, regional and local studies that included irrigation in Earth system models already demostrated the effects of irrigation in different variables. Some regional and local simulations have studied the irrigation impact in some parts of Europe with simulations limited to the duration of one growing season. Therefore, long-term irrigation simulations that cover the whole European continent are still missing. This study quantifies the long-term impact of irrigation on surface and atmospheric variables over the EURO-CORDEX domain using convection-permitting ICON simulations that cover a period of 12 years. Our findings indicate that the magnitude of the irrigation impact is limited by the irrigated region and the year of study in the EURO-CORDEX domain, showing that the land-atmosphere coupling is key to determine the irrigation effects. For instance, the cold and wet summer of 2017 in south Europe weaked the irrigation cooling in the Alps. In contrast, the heat wave of 2018 in Central Europe enabled the influence of irrigation on surface variables in this region.

1 Introduction

The role of irrigation in research has grown significantly since the early 2000s, leading to the integration of irrigation in coupled Earth system models (ESMs) with results that demonstrate its crucial interaction with various components and processes of the Earth system (McDermid et al., 2023). Numerous authors have already mentioned that land representation, which includes irrigation, should be considered in climate modeling on regional and local scales (Fan et al., 2025; Udina et al., 2024; Lunel et al., 2024; Asmus et al., 2023; Lo et al., 2021; Chen and Dirmeyer, 2019), since the absence of irrigation can lead to certain biases (Qian et al., 2020; de Vrese and Hagemann, 2018) and land misrepresentation. To overcome this lack, early research included irrigation in EMS in long-term simulations. However, most of these studies applied coarse resolutions (Valmassoi and Keller, 2022). For example, Cook et al. (2015) employed a resolution of 2°×2.5° latitude/longitude, while Chen and Dirmeyer (2019) used 1.9°x2.5°, and Thiery et al. (2020) applied a horizontal resolution of 0.9°x1.25°. These last two studies used the Community Earth System Model (CESM) for their global simulations. Chen and Dirmeyer (2019) results revealed that irrigation cooling is influenced by land-atmosphere interactions. While Thiery et al. (2020) found that daytime temperatures in the hottest month have increased less in regions with significant irrigation growth. Cook et al. (2015) found that this irrigation cooling is mainly regional and more visible in specific regions such as the Mediterranean, where Thiery et al. (2017) reported

https://doi.org/10.5194/egusphere-2026-3354
Preprint. Discussion started: 10 July 2026

a cooling of -0.24 K. Despite the significant findings of these simulations, their coarse resolution might fail to adequately capture the heterogeneity of the land surface (McDermid et al., 2023), particularly in the intensively irrigated regions of Europe (Valmassoi and Keller, 2022). Thus, we need to account for the fact that the model's resolution may significantly affect the intensity of local cooling (Chen and Dirmeyer, 2019).

Indeed, more recent studies have investigated the irrigation effect on higher resolutions in Europe, such as in the Po Valley, Italy at 3 km horizontal resolution (Valmassoi et al., 2020b) and south-west Europe at ∼12 km horizontal resolution (Asmus et al., 2023). They found a higher temperature decrease than Thiery et al. (2017) in these regions in July, reporting -3 K and -0.68 K, respectively. However, the magnitude of the irrigation effect does not depend solely on the model resolution, but also on how irrigation is parameterized. Although, both irrigation experiments in Europe applied the same irrigation map from Siebert et al. (2013), they employed different EMSs and irrigation settings. Therefore, results over similar regions might differ. On one hand, Valmassoi et al. (2020b) worked with the Weather Research and Forecasting (WRF) and developed three parameterizations with a fixed irrigation amount and schedule (CHANNEL, SPRINKLER and DRIP). On the other hand, Asmus et al. (2023) employed the Regional Climate Model (REMO2020) and implemented a parameterization that adds water directly to the soil. Irrigation is activated when soil moisture falls below an irrigation threshold, while the irrigation volume calculation is based on reaching a specific soil moisture target. Indeed, similar activation schemes exist in some irrigation parameterizations in other land surface models (Lawston-Parker et al., 2023; Leng et al., 2017; Qian et al., 2013). However, Lawston-Parker et al. (2023) and Zappa et al. (2024) emphasize that irrigation activation and estimates are also influenced by human behavior, since farmers determine the timing and quantity of irrigation according to local and regional water management policies, such as water turns and other regulations enforced by irrigation consortiums. Establishing irrigation settings is inherently complex; therefore, Zappa et al. (2024) suggests that irrigation parameterizations should incorporate some specific parameters a-priori.

Other high-resolution simulations implemented constant irrigation rates, similar to Valmassoi et al. (2020b), in the Ebro basin (Lunel et al., 2024). In these simulations, local irrigation information determined the irrigation amount rather than country-level data. Udina et al. (2024) also applied some local irrigation settings in their irrigation simulations for the same basin. In these studies, obtaining local information was possible, since both aimed to compare their findings with in-situ observations collected during the Land Surface Interactions with the Atmosphere over the Iberian Semi-arid Environment (LIAISE) field campaign. Moreover, conducting simulations at highly localized scales allowed Lunel et al. (2024) to reach a horizontal resolution of 400 m using an EMS (Meso-NH v5.5.1 coupled with SURFEX v8.1). These and other local simulations (Valmassoi et al., 2020b; Pop et al., 2025) in Europe mainly focused on short periods spanning from one growing season to several days. And, while these short-term local simulations demonstrated that incorporating irrigation into EMS improves model performance by reducing warm and dry biases, no high-resolution studies have investigated the irrigation effects in long-term simulations at larger scales yet. On a European scale, both the Mediterranean and other regions require long-term irrigation studies to assess interannual impacts, particularly as droughts and heatwaves become more frequent across the continent (Hoy et al., 2020).

Rainfed agriculture is more common in Central and Northern Europe; however, irrigated areas in these regions are increasing. For instance, the irrigated area in Germany experienced a significant increase of 36% in 2019 compared to the area in 2009 (Wenzel et al., 2022), and this trend is projected to persist in the future (McNamara et al., 2024). Indeed, irrigation im-

https://doi.org/10.5194/egusphere-2026-3354
Preprint. Discussion started: 10 July 2026

plementation in recent years served as an adaptation strategy against droughts to lower yield losses (Deb et al., 2022). Given the significance of understanding how land conditions influence the development of droughts and heat waves (Miralles et al., 2019), along with the potential of irrigation practices to mitigate regional heat extremes (Chen and Dirmeyer, 2019), it is essential to conduct further research linking these areas.

Our study aims to fill the gaps highlighted above by quantifying the long-term impact of irrigation on surface and atmospheric variables over the EURO-CORDEX domain using convection-permitting ICON simulations that cover the period 2010–2022. Through this study, we evaluate the inter-annual and seasonal changes in surface variables by comparing irrigated and non-irrigated simulations. In addition, we assess the irrigation effect during two heat waves and evaluate the model output against quality-controlled observations for 2-m temperature and relative humidity.

2 Methodology

2.1 Irrigation implementation

The basis for this implementation is the CHANNEL scheme developed by Valmassoi et al. (2020b) for the WRF model. According to their method, evaporation sources include soil and surface water. We also applied this principle in the present study since our approach integrates irrigation water into grid-scale precipitation before this variable is passed to the land surface model (LSM). We used equation 1 from Valmassoi et al. (2020b) to calculate the irrigation water for each irrigation episode.

$$W_1 = \frac{V_1}{h_1} * T_1 \tag{1}$$

where W_1 is the irrigation water amount in mm s^{-1}. V_1 is the daily irrigation amount in mm d^{-1}, h_1 is the number of irrigation hours in seconds and T_1 is the irrigation interval (absolute number of days).

Unlike the original CHANNEL scheme, the current parameterization has a daily irrigation volume (V1) equal to the readily available water (RAW) Eq. 2 (Allen et al., 1998). RAW is the portion of the total available water (TAW) that a crop can absorb from the root zone without experiencing any water stress. To calculate RAW, we also need information related to the depletion fraction (ρ). This variable is a crop-specific parameter that depends on potential evapotranspiration (Eekhout et al., 2024). However, Brekel et al. (2023) mentions that utilizing a fixed depletion fraction value is also feasible. We chose this approach because the LSM in ICON does not distinguish between different crops types yet. Therefore we adopted a constant value of 0.65.

$$RAW = TAW * \rho \tag{2}$$

where RAW is the readily available water in mm. TAW is the total available water in mm and ρ is the depletion fraction.

TAW calculation includes soil moisture thresholds (field capacity and permanent wilting point) from a specific soil type of a given grid-cell as shown in Eq. 3. Additionally, for our calculations, TAW units should be in mm of water. To achieve

https://doi.org/10.5194/egusphere-2026-3354
Preprint. Discussion started: 10 July 2026

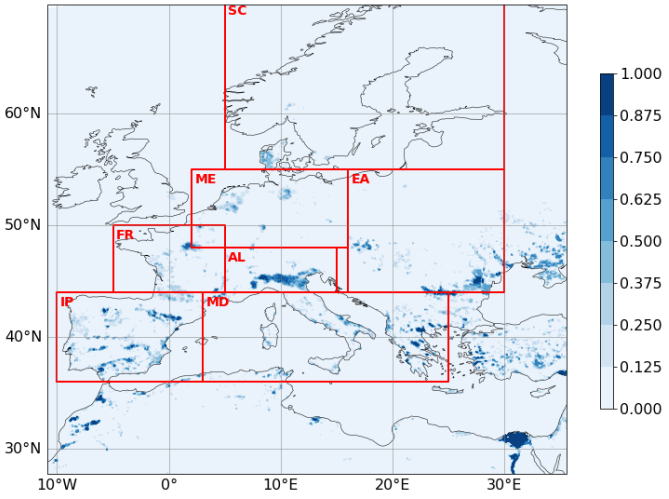

Figure 1. Adapted Irrigation fraction from Siebert et al. (2013) to ICON unstructured grid. Red squares indicate Prudence regions in the EURO-CORDEX domain.

this, TAW calculations usually consider the specific crop root depth values. However, due to the limitations of our LSM, our parameterization considers a constant value for this variable.

$$TAW = (\theta_{fc,i} - \theta_{pwp,i}) * \text{root\_d} \tag{3}$$

where TAW is the total available water in mm. θ_{fc} is the soil field capacity, θ_{pwp} is the soil permanent wilting point and root_d is the root depth in milimeters.

2.1.1 Irrigation map

We used irrigation data from Siebert et al. (2013), Digital Global Map of Irrigation Areas to version 5. This data set derives from statistical information from census and studies related to irrigation at the national and subnational level from the period 2000–2008. The quality control conducted on this data set showed good scores for different countries in Asia, for Northern America and Southern and Western Europe. The horizontal resolution is 0.083333°, which is approximately 9.24 km at mid-latitudes. We adjusted and adapted this map to ICON's characteristics in terms of horizontal resolution and triangular grid through first order conservative remapping using the Climate Data Operators software, which implements conservative remapping through the YAC library (Taylor, 2024). Then, we modified ICON's default land cover map and focused on the category "irrigated croplands" to introduce the adapted Siebert et al. (2013) dataset, which is displayed in Figure 1. From the original map, we took into account only those grids with more than 10% of irrigation fraction.

https://doi.org/10.5194/egusphere-2026-3354
Preprint. Discussion started: 10 July 2026

2.1.2 Irrigation season, time and frequency

To coincide with the crop season, we based our settings on literature. From three crop calendars (maize, wheat and rice) available for European countries (JRC.D.5, 2015), we focused on maize, as it is a crop cultivated in most countries (Zappa et al., 2024; McNamara et al., 2024). Depending on the region, sowing activities concentrate between late April and early May. Moreover, focusing on highly irrigated areas, Rubio-Martin et al. (2020); Azar et al. (2016); Nana et al. (2014) mentioned that some areas of Spain (Jucar River Basin) and Italy (Po Valley - Cremona, Lombardy) have an irrigation period from May to September for some summer crops. Additionally, the growing season for irrigated crops in central Europe, such as Germany, also starts around April with irrigation events taking place mainly in June (Wenzel et al., 2022). Regarding the irrigation settings such as irrigation timing, Zappa et al. (2024) mentioned that they are frequently influenced by various factors rather than being strictly physically-based, and these parameters should be established in advance and Lobell et al. (2009) suggested that irrigation frequency should follow a more realistic schedule rather than daily. With this information, the irrigation settings include an irrigation start date on May 1st of each year, an irrigation start time at 5 UTC and an irrigation length of 5 hours. The irrigation frequency is 12 days and the last irrigation event takes place on August 17th of each year. Therefore, our irrigation period takes place on the summer crop season in Europe, season when the effects of irrigation on the atmospheric component are more evident as atmospheric conditions are warm and dry (Valmassoi et al., 2020b; Thiery et al., 2017; Zeng et al., 2017).

2.1.3 Irrigation amount

Having a fixed irrigation amount showed a good performance in simulating the weather on local scales (Valmassoi et al., 2020b). However, we had to find an approach that also performs well on regional scales. McNamara et al. (2024) found that not only the climatic water availability or the crop type determine the irrigation demand, but also soil characteristics such as the water retention capacity. Therefore, our irrigation amount is calculated based on soil information of a specific grid cell, as stated in Eq. 2. To apply this equation, we also need some constant parameters such as depletion fraction and root depth. Bos (2004) mentioned that typical depletion fraction values are in the range between 0.5 and 0.8. Therefore, We decided to use the average of this range, 0.65. Regarding root depth, we opted to work with 810 mm, a value that is in between the range of 800 and 1200 mm of maximum effective rooting depth for Maize (Allen et al., 1998). Field capacity and permanent wilting point values come from a reference table with soil parameters in the land surface model data. Table 1 shows reference irrigation amounts calculated based on soil types available in the default soil map. These amounts change when precipitation is present in the irrigated area, as a result, the irrigation amount is not constant as seen in the Supplementary material Figure A1, which shows yearly average irrigation amount per prudence region considering the irrigation fraction.

2.2 Model Set-up

We ran two simulations with the operational ICON-nwp in Limited Area Mode on the EURO-CORDEX domain, one control and one irrigation experiment, both at 3 km resolution. Input data to run these simulations include initial and boundary conditions from the new reanalysis ICON-DREAM, 13 km horizontal resolution and hourly output (Valmassoi et al., 2025). We

https://doi.org/10.5194/egusphere-2026-3354
Preprint. Discussion started: 10 July 2026

Variable	Sand	Sandy loam	Loam	Clay loam	Clay
fc	0.196	0.26	0.34	0.37	0.463
pwp	0.042	0.1	0.11	0.185	0.257
RAW	81.08	84.24	121.10	97.40	108.46
10 events	810.81	842.40	1210.95	974.03	1084.59

Table 1. Reference irrigation amount in mm based on soil type moisture thresholds. Values for fc and pwp come from ICON-nwp soil lookup table. RAW values are calculated with Eq. 2 and ρ=0.65, root_d=810 mm.

used a similar namelist as described in Roque and Valmassoi (2025). The control run started on January 01, 2010, 00UTC and ran until December 31, 2022, 21UTC. The irrigation experiment started from a restart from the control run on May 1, 2010, 05UTC and consists of a total of 10 irrigation events per year. All post-processing data for spatial and temporal means include the period 2011–2010, being 2010 the spin-up year.

2.3 Climate means, timeseries and extremes

To ensure the robustness of our results when showing the mean climate summer over the entire simulation period, we employed two statistical approaches: a paired test and a field significance test for our 12 year simulation. Similar methods were previously applied by Lorenz et al. (2016) in the context of land-use change (e.g., deforestation) impacts on climate variables such as temperature and precipitation. We used the Student's t-test on two related samples (ttest_rel in SciPy) with a significance level of 0.05 to assess whether the differences between the irrigation and control experiments are statistically different from zero. To address spatial correlation and reduce the risk of false positives, we applied the False Discovery Rate (FDR) following the Benjamini–Hochberg (Benjamini and Hochberg, 1995) (fdrcorrection in statsmodels) procedure as a field significance test, as recommended by (Wilks, 2006) for meteorology and climatology evaluation.

To assess the temporal impact of irrigation, we selected only irrigated grids per prudence region and calculated the difference between irrigation and control experiments, focusing on monthly averages. Moreover, we include the temporal standard deviation to these monthly mean differences. This analysis included key variables such as soil moisture, latent and sensible heat fluxes, 2-meter temperature, and radiation outputs. The selected prudence regions for this study were the Alps, Mediterranean and Mid-Europe (Figure 1).

Given the importance of assessing the effects of land-use change on the atmosphere during droughts and heatwaves (Miralles et al., 2019), it was crucial to consider extreme cases in our irrigation study. The frequency and intensity of heat waves during our study period are notable. For instance Hoy et al. (2020) mentions the years 2013, 2015, 2017, 2018 and 2019 as years with intense heatwaves that affected different regions of Europe at various timescales. Moreover, considering the last 43 years, the most severe heat wave in Southwest Europe occurred in 2022 (Kim et al., 2024). From these extreme events, we focused on two that cover two different regions: 2017 in southern Europe and 2018 in central Europe. The event of 2017 surpassed the 2003 heat wave, reaching an average peak of 34.4°C in southeast Europe during the window of 3–5 August (Kew et al., 2019).

https://doi.org/10.5194/egusphere-2026-3354
Preprint. Discussion started: 10 July 2026

Asmus et al. (2023) already studied this event in the context of irrigation and it serves as a reference for comparison. Therefore, we chose a similar period and region, from August 1st to August 16th in the Alps. In central Europe, 2018 was characterized not only by high temperatures, but also by an extended drought (Rousi et al., 2023; Ionita et al., 2021; Moravec et al., 2021). The study from Rousi et al. (2023) shows that the heat wave in this region started on July 23rd and lasted until August 9th. From this reference, we focus on Mid-Europe for the period July 20th to August 4th.

2.4 Validation and evaluation

The validation of our simulation is done against 3 hourly quality-controled observations from ICON DREAM reanalysis. We focus on temperature 2-m and relative humidity, as these variables are often associated with biases related to the misrepresentation of irrigation in weather and climate modeling. To asses the specific impact of irrigation, from all observations available, we selected those located in irrigated areas and calculated the monthly biases and root mean square error (RMSE) from May to September. Further, we calculated these metrics per prudence region, which are shown in the Figure 1, since this allows us to evaluate the model performance per representative regions in Europe.

3 Model discussion

3.1 Prudence regions

We evaluated all observations available per prudence region from May to September (2010-2022) in the Alps, Mediterranean, Iberian Peninsula and Mid-Europe. On a prudence region scale, the T2m bias reduction in the irrigation simulations in the Alps and Mediterranean reached on average -0.18 K for MJJAS in both regions (Figure 2a and b). The average bias reduction in Mid-Europe is lower, only -0.06 K. Contrary, the T2m bias increased on average 0.20 K in MJJAS in the Iberian Peninsula. We observed a similar pattern for relative humidity (RH), a bias reduction in the Alps, Mediterranean (Figures 2c and d) and Mid-Europe, whereas in the Iberian Peninsula a bias increament. This bias increament in the Iberian Peninsula is explained in the next section. Regarding the analysis of individual monthly biases for T2m, we found significant improvements especially from July to September in the Alps, while for the Mediterranean, the results are significant from May to August. For Mid-Europe and the Iberian Peninsula all absolute monthly bias differences are significant (Table 2). This individual analysis for RH also shows significant improvements for all evaluation months in the Alps and the Mediterranean. However, in the Iberian Peninsula, RH biases reduction are significant only for July and August (Table A1).

https://doi.org/10.5194/egusphere-2026-3354
Preprint. Discussion started: 10 July 2026

(a) Alps – T2m

(b) Mediterranean – T2m

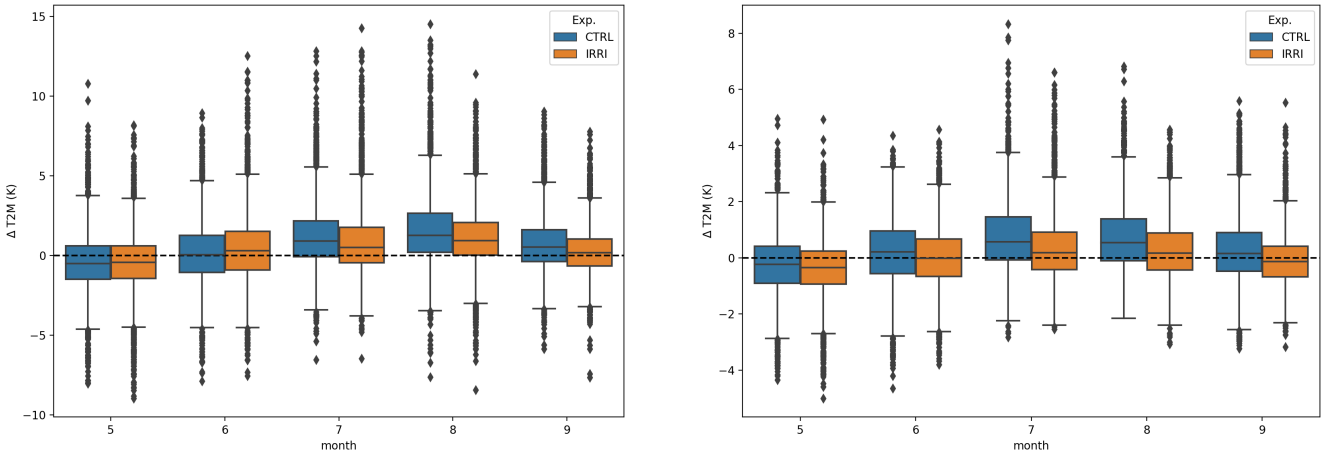

(c) Alps – RH

(d) Mediterranean – RH

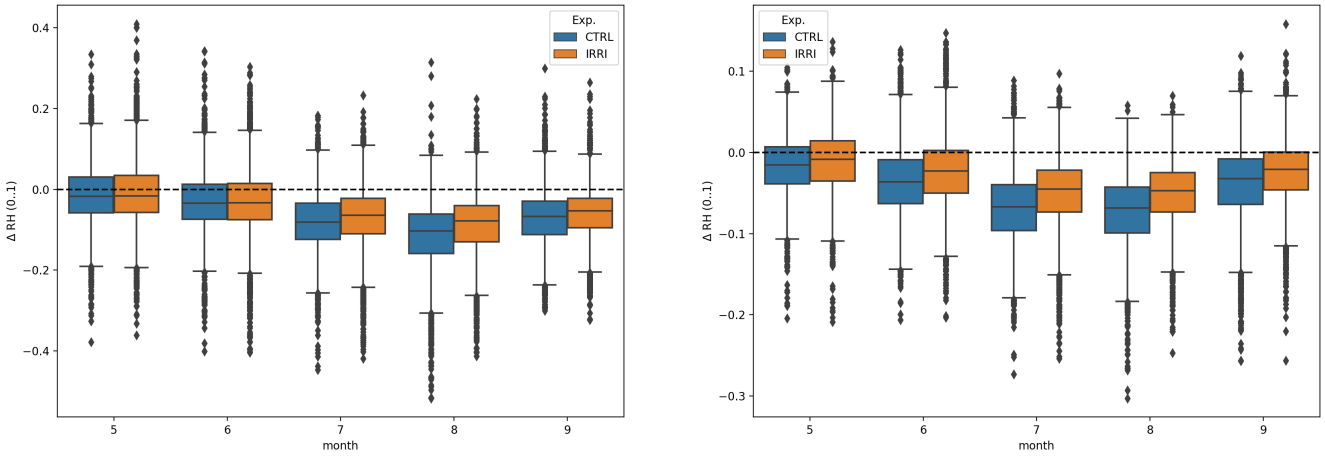

Figure 2. Boxplot of monthly 2-m Temperature and Relative humidity biases for control and irrigation experiments against observations for the Alps and Mediterranean.

https://doi.org/10.5194/egusphere-2026-3354
Preprint. Discussion started: 10 July 2026

Region	Exp.	May	June	July	August	September
Alps	CTRL	-0.50	0.06	0.91	1.26	0.54
	IRRI	-0.42	0.30	0.51	0.94	0.19
	ABS	-0.08	0.24*	-0.40*	-0.32*	-0.35*
Mediterranean	CTRL	-0.24	0.21	0.57	0.54	0.15
	IRRI	-0.34	-0.01	0.18	0.16	-0.13
	ABS	0.11*	-0.20*	-0.39*	-0.38*	-0.02
Iberian P.	CTRL	-0.62	-0.38	-0.20	-0.31	-0.40
	IRRI	-0.75	-0.52	-0.49	-0.59	-0.56
	ABS	0.12*	0.14*	0.29*	0.29*	0.16*
Mid-Europe	CTRL	-0.80	-0.15	0.27	0.37	-0.04
	IRRI	-0.81	0.03	0.09	0.34	-0.08
	ABS	0.01*	-0.13*	-0.18*	-0.02*	0.04*

Table 2. Control and irrigation biases from May to September considering all observations present in each Prudence region for 2-m Temperature. ABS is the absolute difference between IRRI and CTRL.
(*) Statistically significant change in the bias due to irrigation (5% significance level on two-sided Wilcoxon signed rank test on multi-annual data).

3.2 Irrigated areas

We filtered all observations available to include only those that are located in or maximum on a radius of 10 km of irrigated grids. In general, we found a bias improvement for T2m in the Alps and Mediterranean in most months throughout the simulation period (Figure 3a and b). Especially for July, August and September in the Alps, when the average relative bias reduced by 0.69, 0.65 and 0.86 K respectively. In the Mediterranean, the average relative bias reduction for these months was 0.69, 0.81 and 0.56 respectively. However, the initial irrigation month, May, showed a bias deterioration in most years in both regions. These results might be influenced by the initial irrigation date, May 1st in our experiments, as well as the irrigation frequency, which could also contribute to these findings. The irrigation scheduling we applied is fixed, however, in reality this varies year to year and we might fail to represent these dates correctly, especially for the month of May and in some cases in June. Therefore, as also recognized by Zappa et al. (2024), even though irrigation parameterizations in Earth system models exist, we still lack essential information about the distribution of irrigated areas, the timing of irrigation, and the volume of irrigation water.

Similarly to the evaluation on a prudence region scale, the evaluation on irrigated areas in the Iberian Peninsula showed a bias increase in all evaluation months (Table A2). This bias deterioration may be linked to the irrigation scheduling, since Lunel et al. (2024) and Altés et al. (2023) reported that fields in the Ebro basin are irrigated during the early night hours to prevent

https://doi.org/10.5194/egusphere-2026-3354
Preprint. Discussion started: 10 July 2026

water losses due to the high diurnal temperatures. In contrast, our irrigation time starts at 5 UTC. Another reason for the bias increment might be related to the irrigation type, since different irrigation types coincide in the irrigated area of the Ebro basin, from flood to drop and sprinkler irrigation (Zappa et al., 2024). In the Ebro basin, Lunel et al. (2024) obtained a bias and RMSE reduction from 7.40°C to -2.94°C and 10.90°C to 5.53°C when using an approximate water suply and irrigation scheduling based on the field work information. Therefore, the implementation of appropriate irrigation settings can also reduce the biases and RMSE in the irrigated areas of Spain.

Table A2 also shows that the irrigation bias reduction in Mid-Europe is only significant for two months, July and August. In this region, the number of irrigation events and the irrigation amount is usually lower than in southern Europe. For instance, Wenzel et al. (2022) studied the impact of irrigation levels on potato production in North Germany and reported an average irrigation amount of 24.4 mm per irrigation event and a number of irrigation events of 5 (total irrigation level of 122 mm. For 2021, we added an average of 72.8 mm $year^{-1}$ in Mid-Europe). They also mentioned that precipitation alone did not fulfill the crop water requirements in 2021, therefore, irrigation was indeed needed and found that a total of 94.8 mm was the optimum irrigation amount for this crop. Therefore, even though warmer years, such as 2018, need more irrigation water and events, the irrigation scheduling and amount that our parameterization applied for this region needs an adjustment. Regarding the RMSE, Figures 3c and d show that the relative RMSE change also reduces in nearly all months and years, indicating an improvement of the model performance in Alps and Mediterranean.

https://doi.org/10.5194/egusphere-2026-3354
Preprint. Discussion started: 10 July 2026

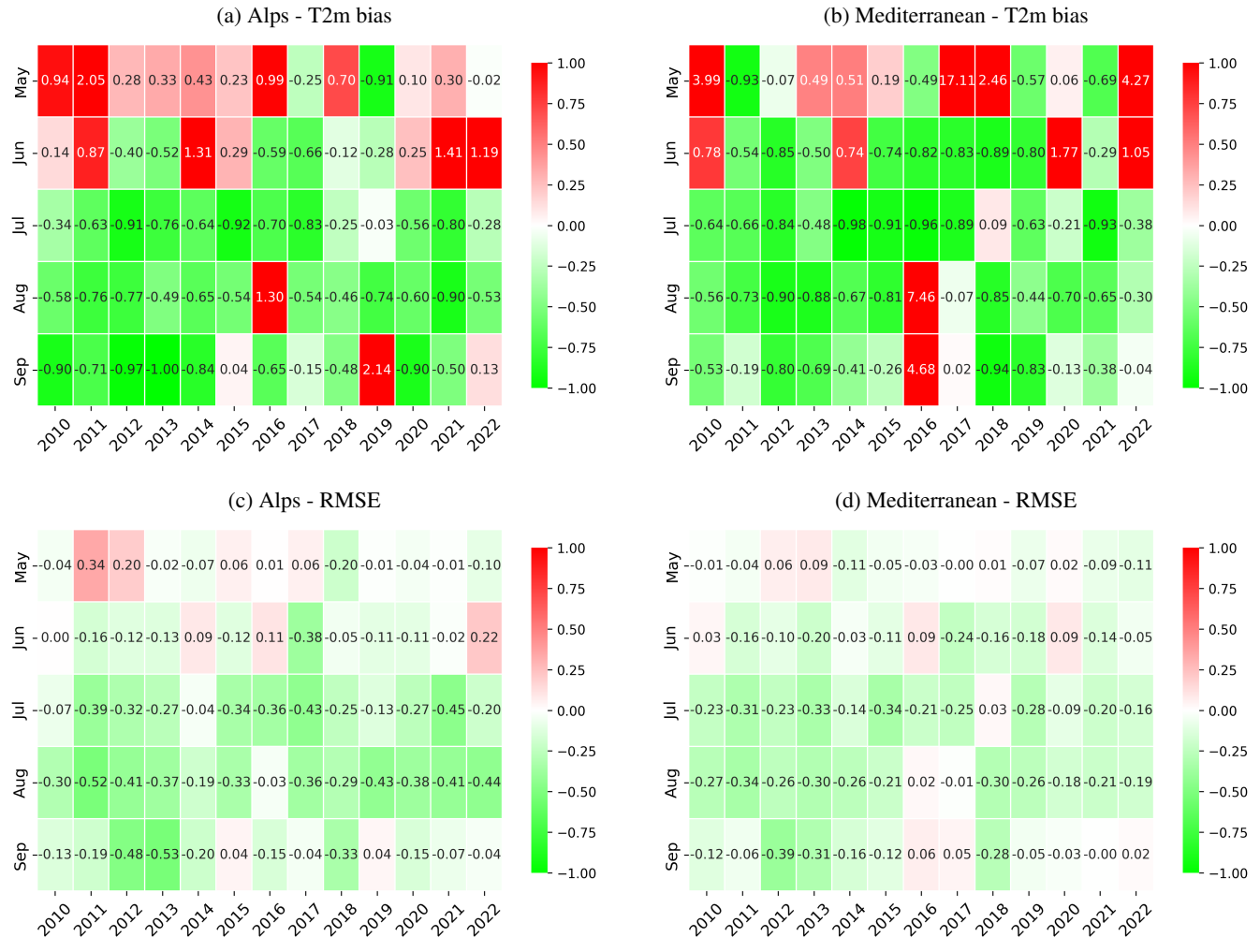

Figure 3. Relative difference for bias and RMSE [(abs(IRRI) - abs(CTRL))/abs(CTRL)] for 2-m temperature.

Our evaluation expresses relative humidity as a fraction between 0 and 1, as a result, the absolute biases are small (<0.1) and the relative bias difference can be amplified. Mentioning this, the bias improvement of relative humidity is more consistent through most months and years than T2m since only May has a bias deterioration in some years for the Alps and Mediterranean (Figure 4a and b). The average relative difference in the biases between irrigation and control experiments for the evaluation period shows an improvement of 0.40 and 0.55 across all months for Alps and Mediterranean respectively. This reduction is also visible and statistically significant in the Iberian Peninsula and Mid-Europe, but only for July and August and from July to September respectively (Table A3). The other months show a relative bias increase in these regions. Similar to the relative bias difference, the relative RMSE change (Figures 4c and d) is mostly negative, showing an overall error reduction in the Alps and Mediterranean.

https://doi.org/10.5194/egusphere-2026-3354
Preprint. Discussion started: 10 July 2026

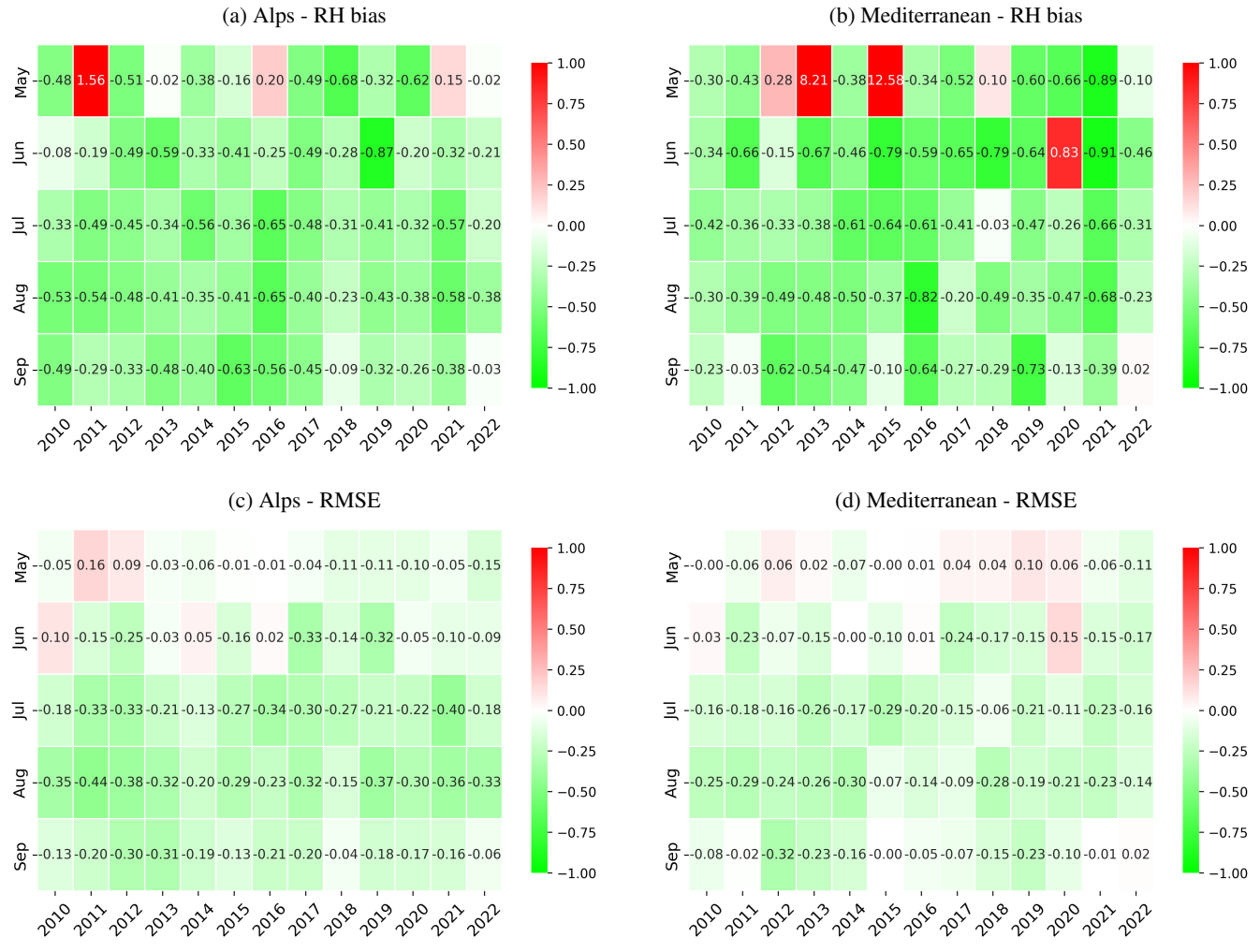

Figure 4. Relative difference for bias and RMSE [(abs(IRRI) - abs(CTRL))/abs(CTRL)] for relative humidity.

4 RESULTS AND DISCUSSION

4.1 Influence of Irrigation on the Climatological summer mean

As stated in the Sect. 2, irrigation started on May 1st of each year. As a result, in the current section we focus on the climatological mean of May, June, July, August and September. In May, the irrigation effect on soil moisture (sm) covered most of the irrigated areas in Europe with a limited effect in central and northern Europe (Figure A2a). On average, irrigation in May increased sm values in 2.66 (± 1.47) kg m^{-2} over irrigated areas. The average increase for JJA was 2.45 (± 1.50) kg m^{-2}. This is slightly lower than May, however, the effect in JJA is visible in all irrigated areas across Europe (Figure 5a). Eventhough irrigation stops on August 17th, sm signal is still evident in September (Figure A2b), showing that sm memory induced by

https://doi.org/10.5194/egusphere-2026-3354
Preprint. Discussion started: 10 July 2026

irrigation, can persist for several weeks to months (Koster et al., 2000), indicating a delayed effect of irrigation at this scale (Qian et al., 2013). On average, sm increased in 1.86 (± 0.82) kg m^{-2}.

The influence of sm increments altered the partitioning of the surface energy fluxes. Under irrigation, normally the net radiation at the surface is primarily partitioned through latent heat flux (LHF), rather than sensible heat flux (SHF) (Benson and Dirmeyer, 2021). In May, similarly to soil moisture, LHF values increased mostly for southern Europe (Figure A3a) with an average of 29.93 (± 21.27) W m^{-2}. In an opposite direction, the decrease in SHF was slightly lower than the LHF increase (Figure A3c), with an average value of 26.86 (± 18.48) W m^{-2}. In the summer season this difference enhances since LHF raised more than the SHF decrease. This is visible in Figures 5b and 5c. The increase of LHF is higher over southern Europe than over the north, the average increase is 34.81 (± 22.60) W m^{-2}. The irrigation effect on the drop of SHF is consistent over the whole irrigated areas in the EURO-CORDEX-domain, as this variable decreases on average in 28.40 (± 19.01) W m^{-2}. In September, LHF continues dominating the energy decrease over SHF (Figure A3b and A3d), however, in a lesser extent than in summer. On average, LHF increased in 19.83 (± 10.28) W m^{-2} while SHF decreased in 17.19 (± 8.73) W m^{-2}.

In May, the average evapotranspiration (ET) increase over irrigated areas is 32.05 (± 22.79) kg m^{-2} (Figure A4a). In summer, the magnitude of ET increase is much higher than LHF, as this value reached on average 110.81 (± 89.71.91) kg m^{-2}. The field campaign, LIAISE (July 2021), in Spain also reported a large evapotranspiration increments, since the cumulative evapotranspiration was ten times higher at the irrigated site compared to the rain-fed site (Brooke et al., 2024). The higher increase we found is also related to our irrigation approach, since we add irrigation water to the grid-scale precipitation and more water is available in the interface for ET. Yang et al. (2019) also found that under such conditions (irrigation water at the surface), water either evaporates or turns into surface runoff, rather than infiltrating into the soil. In Figure 5d, we found an ET decrease over north Germany, which is consistent with changes in LHF and SHF over the same area, since LHF slightly decreases and SHF increases. In September, since no irrigation took place, the effect on ET decreases, but it is still present. The average ET increment was 20.55 (± 10.66) kg m^{-2}.

https://doi.org/10.5194/egusphere-2026-3354
Preprint. Discussion started: 10 July 2026

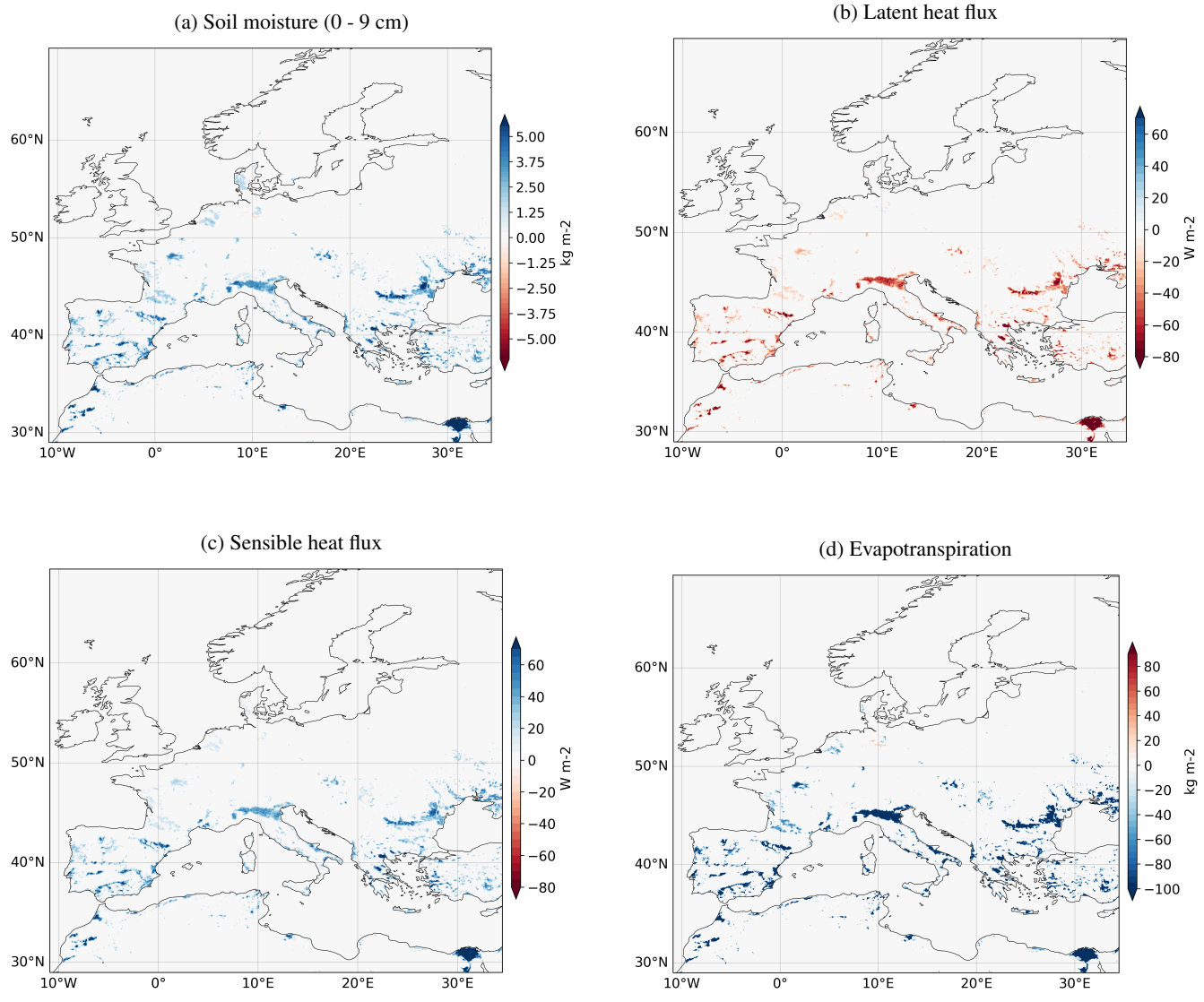

Figure 5. Seasonal mean differences for JJA (2011-2022) for different variables.

The irrigation impact on soil moisture and energy fluxes showed in the previous paragraphs also influenced the climatological mean of 2-m temperature (T2m). Even though there was an evident impact for these variables in May, the impact in T2m is visible only in few locations in Spain and the large irrigated areas of Egypt (Figure A5a). The average T2m cooling in these areas was 0.71 (± 0.41) K. The cooling effect expanded to all the Mediterranean, parts of France and Eastern Europe for the summer season (Figure 6a), with an average value of 0.78 (± 0.44) K. Across the 12 years of simulation, when considering

https://doi.org/10.5194/egusphere-2026-3354
Preprint. Discussion started: 10 July 2026

the two significance test, the cooling effect is not significant in September (Figure A5b). However, if we only consider the the Wilcoxon Signed-Rank test, there are still plenty of irrigated areas in southern Europe that show a cooling effect (Figure A6).

The changes in T2m are linked with radiation shifts. In May, the upward longwave radiation (ULR) decreased on average 7.86 ($\pm$ 5.12) W m^{-2}, this is visible in most irrigated areas of southern Europe, except in the Alps region where there is not significant effect (Figure A7a). In summer, not only ULR decreases, but also the downward longwave radiation (DLR) reduces in some irrigated areas. ULR follows the same T2m cooling spatial pattern with a reduction of 8.63 ($\pm$ 5.24) W m^{-2} (Figure 6b). The irrigation effect on DLR is located specifically in small irrigated areas in southern Europe with an average decrease of 1.79 ($\pm$ 1.90) W m^{-2} (Figure A8b) and a limited increase in some areas around the Alps. In September, the ULR reduction dimineshes to 6.54 ($\pm$ 3.01) W m^{-2} with an impact area similar to May (Figure A7b).

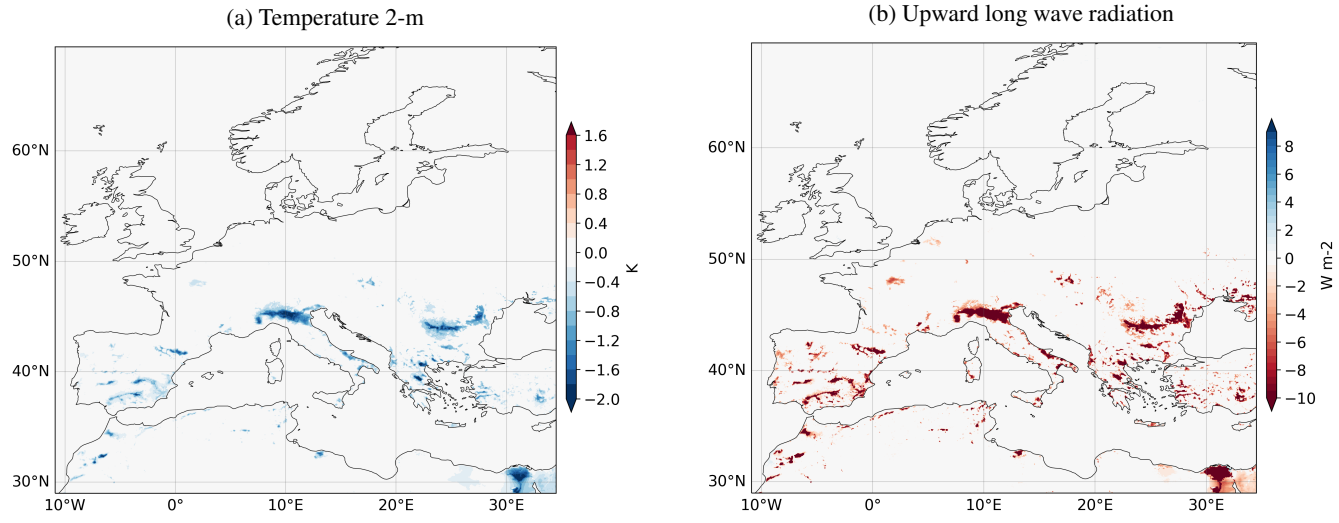

Figure 6. Seasonal mean differences for JJA (2011-2022) for different variables.

4.2 Temporal and spatial mean impact in irrigated areas

When analyzing the climatological mean of various variables, we observed that the irrigation effect exhibited different magnitudes in surface variables, influenced by both spatial and temporal factors. For instance, irrigation attained a consistent impact increasing soil moisture across the entire EURO-CORDEX domain. However, other surface variables such as LHF or EVAPT exhibited heterogeneous seasonal patterns between the northern and southern regions. Therefore, in the current section we present monthly averages in irrigated areas per prudence region for different surface variables, in order to explain the impact per representative region.

https://doi.org/10.5194/egusphere-2026-3354
Preprint. Discussion started: 10 July 2026

4.2.1 Soil moisture

The soil moisture increment during the irrigated period (MJJA) is consistent across all prudence regions (Figure 7), however, the magnitude of this increase differs per region. For instance, the Mediterranean region attained the highest percentage of sm increament with an average of 25.39% (1.72 ±0.36 kg m^{-2}) (Figure 7b). For this period, the Alps region achieved on average 23.65% (2.03 ±0.79 kg m^{-2}) of increase (Figure 7a), while Mid-Europe is the regions with the lowest sm increment, only 10.74% (0.90 ±0.67 kg m^{-2}) on average (Figure 7c).

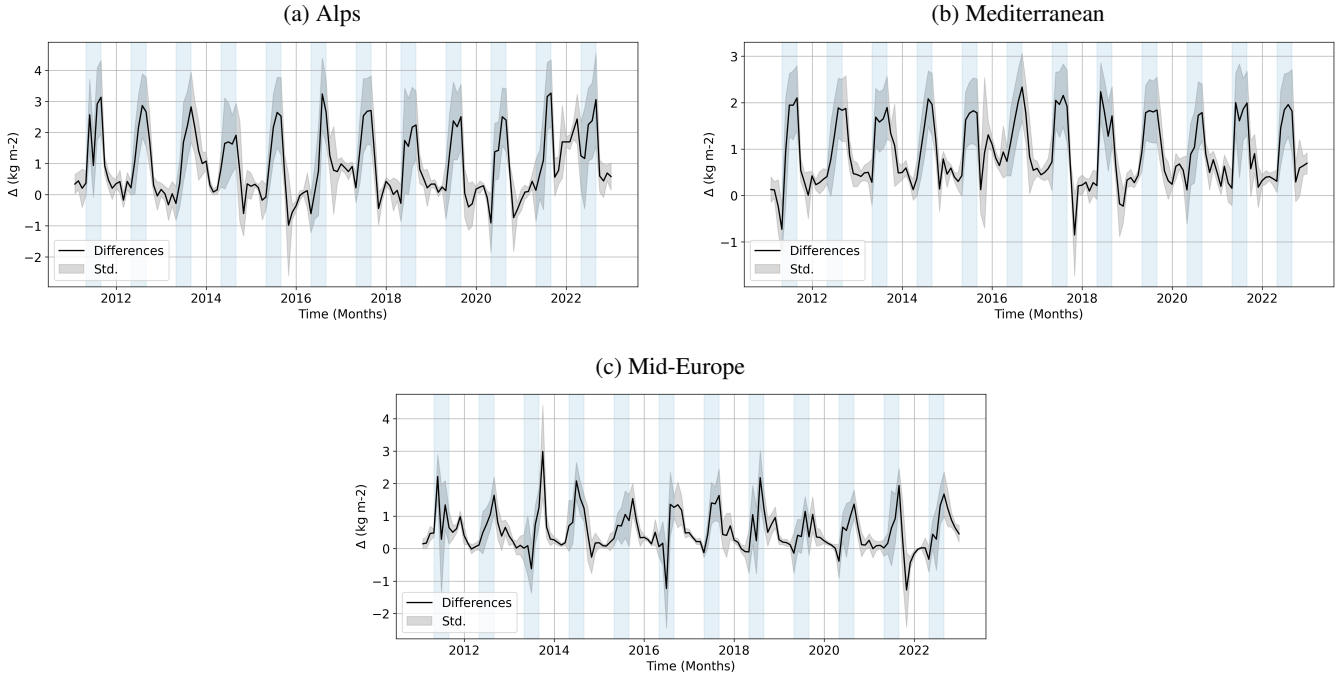

Figure 7. Timseries of monthly mean differences per prudence region, irrigation minus control, for soil moisture (0 - 9 cm). Blue shading indicates the irrigation period, from May to August of each year.

4.2.2 Energy fluxes

Evaluating LHF and SHF we can notice some noteworthy events in the Alps, Mediterranean and Mid-Europe. In the Alps, LHF obtains an average increase in MJJA of 40.73% (27.99 ± 17.48 W m^{-2}), while SHF decreases on average 37.21% (20.77 ± 13.18 W m^{-2}) (Figure 8a). From its whole timeseries, three years outstand: 2014, 2017 and 2022, which correspond to specific events. For instance, LHF and SHF corresponding increase and decrease are the lowest of the timeseries in 2014. This is consistent with the unusual cold and wet JJA in southern Europe in 2014 (Ratna et al., 2017), therefore, the normal high land-atmosphere coupling in JJA decreased under low temperatures and high precipitation amounts. During the heat waves of 2017 and 2022 in southern Europe (Kim et al., 2024; Kew et al., 2019), we observe the highest increase and decrease of LHF

https://doi.org/10.5194/egusphere-2026-3354
Preprint. Discussion started: 10 July 2026

and SHF respectively in the Alps and Mediterranean, indicating how such events influence the land-atmosphere coupling and the irrigation effect. In the Mediterranean, the LHF and SHF changes for MJJA are sighly lower than in the Alps, with LHF increasing on average in 54.56% (24.26 ± 8.49 W m^{-2}) and SHF decreasing in 37.82% (19.52 ± 6.36 W m^{-2}) (Figure 8b). Unlike these regions, the irrigation impact in Mid-Europe for MJJA only reached an average of 9.48% (7.15 ± 6.10 W m^{-2}) increase of LHF and a decrease of 7.87% (5.59 ± 6.36 W m^{-2}) in SHF, which is understandable, since this region is usually within the enery-limited regime (Rousi et al., 2023). However, Figure 8c also shows that irrigation significantly affected the energy partitioning during the 2018 heat wave, which is consistent with Rousi et al. (2023) findings that the evaporative regime in Germany changed from energy-limited to moisture-limited. They mentioned that the lack of precipitation enhanced this change. We investigate these events in more detail in the Sect. 4.3.

From Figure 8, it is evident that the increases in LHF are greater than the decreases in SHF in most cases. Wu et al. (2018) also observed a smaller decrease in SHF compared to the increase in LHF. They attributed this to the reduction of Upward Longwave Radiation (ULR) caused by the irrigation cooling effect (Yao et al., 2025; Guillod et al., 2013), which subsequently increased the net surface radiation. Although Qian et al. (2013) mentioned that irrigation alters the partitioning of energy fluxes without affecting the net radiation at the surface, since albedo, longwave emissivity, and surface temperature influence the radiation budget (Shrestha and Simmer, 2020), other authors also found changes in the net radiation. For instance, in the U.S. Yang et al. (2019) detected an increase in net radiation of 13.3 W m^{-2}, due to a decrease in the ULR of 4.9 W m^{-2} with the WRF model. Marcella and Eltahir (2014) observed a greater increase in net radiation, ranging from 25-70 W m^{-2} in irrigation experiments simulated for West Africa. Moreover, this is also evident in field campaigns, such as LIAISE, which took place in Spain in the summer of 2021. Mangan et al. (2023) measurements demonstrated that a rainfed fallow area exhibited higher ULR compared to an irrigated alfalfa area, which in consequence had more available energy. In our study, we also found a reduction in ULR (Figure A9), for MJJA ULR decreased on average in irrigated areas 7.99 (± 6.89), 6.17 (± 3.53) and 1.14 (± 3.35) W m^{-2} in the Alps, Mediterranean and Mid-Europe respectively. However, the net radiation in the Alps and Mediterranean did not increase, contrary it slightly decreased (Figure A10), while in Mid-Europe net radiation increased. Therefore, we also analyzed the Downward Shortwave Radiation (DSR), a variable related with cloud cover changes (Guillod et al., 2013), and found that for MJJA this variable decreased on average -0.83 (± 5.63) W m^{-2} and -0.82 (± 3.31) W m^{-2} in the Alps and Mediterranean respectively (Figure A11). Contrary to our results, Lunel et al. (2025) discovered that irrigation had no significant impact on DSR. They attributed this to minimal cloud cover and the dominance of synoptic-scale conditions. Regarding Downward Longwave Radiation (DLR), we found that it slightly decreased in the Alps and Mediterranean as well (Not shown) due to the atmospheric cooling. Therefore, reductions in DSR and DLR, which reduce the incoming energy at the surface, explain the slight decrease in net radiation over the Alps and Mediterranean. This reduction in incoming radiation dominates over the decrease in ULR resulting from surface cooling, which only partially mitigates the net radiation reduction.

https://doi.org/10.5194/egusphere-2026-3354
Preprint. Discussion started: 10 July 2026

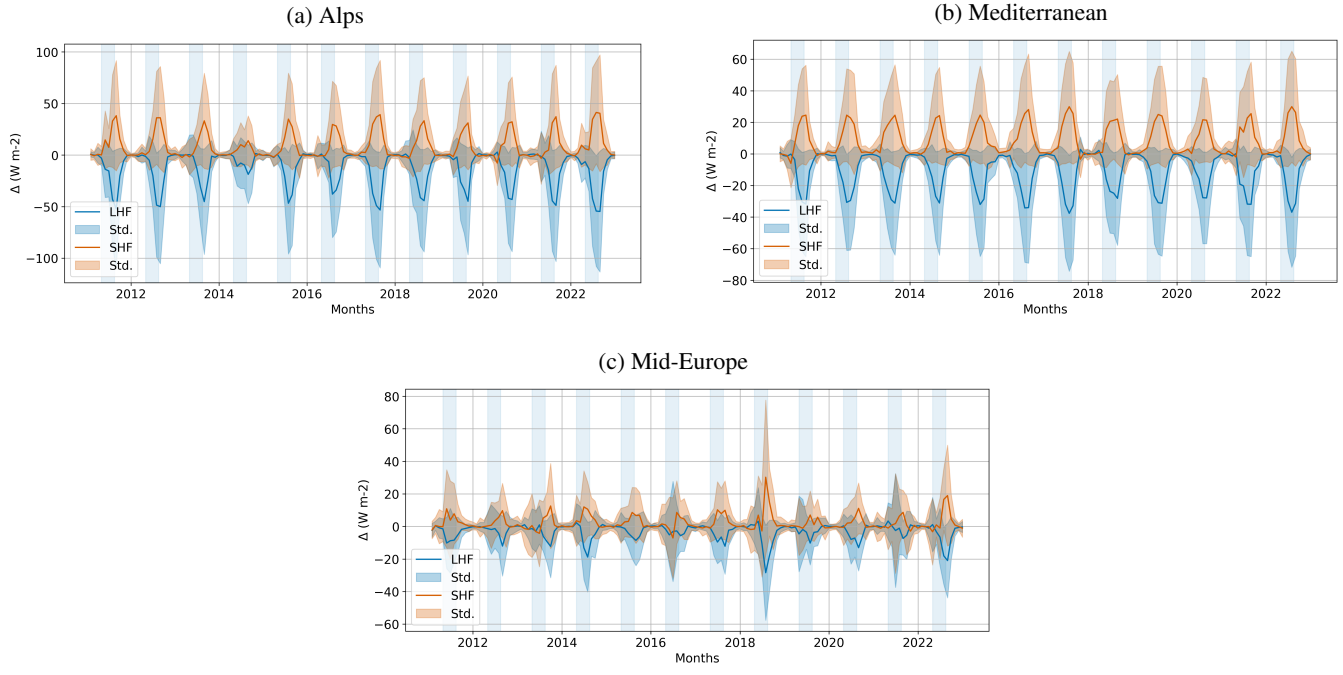

Figure 8. Timseries of monthly mean differences per prudence region, irrigation minus control, for latent heat flux and sensible heat flux. Blue shading indicates the irrigation period, from May to August of each year.

4.2.3 2-meter Temperature

To analyze the irrigation impact on temperature, we focused on T2m, but also on maximum (Tmax_2m) and minimum (Tmin_2m) temperatures. Similar to other studies (Asmus et al., 2023; Valmassoi et al., 2020a; Wu et al., 2018; Sacks et al., 2009), we found a higher irrigation cooling effect for Tmax_2m. In the Alps, the average cooling effect in MJJA reaches -1.08 ($\pm$ 1.10) K for Tmax_2m, while T2m reduces only in 0.82 ($\pm$ 0.86) K (Figure 9a). In their global irrigation simulations, Chen and Dirmeyer (2019) also found daytime cooling in the Po Valley of Italy. A local irrigation simulation in northern Italy developed by Valmassoi et al. (2020a) found a Tmax_2m cooling in the range between 0.75 and 1 K for June and 2.5 and 3 K for July. Asmus et al. (2023) studied the irrigation effect in south-west Europe and reported that Tmax_2m and T2m achieved their peak cooling in July, with -0.68 K and -0.39 K, respectively. In these specific monts, we found a Tmax_2m cooling of 0.45 K in June and 1.67 K in July, with August being the month with the highest cooling, 1.98 K. In the Mediterranean, Tmax_2m and T2m reached a cooling effect of -0.71 ($\pm$ 0.60) and -0.58 ($\pm$ 0.48) K respectively (Figure 9b). In both regions, Tmin_2m also decreases, although the magnitude is much lower, only around -0.23 K on average. Unlike these results, Valmassoi et al. (2020a) found Tmin_2m almost not affected. In the case of Mid-Europe, since this region is characterized by a energy-limited regime, the impact in MJJA is lower than 0.1 for all temperatures (Figure 9c). In fact, Chen and Dirmeyer (2019) already de-

https://doi.org/10.5194/egusphere-2026-3354
Preprint. Discussion started: 10 July 2026

termined that the sensitivity of surface temperature to irrigation is strongly linked to the climate regime of the specific irrigated area.

In the case of the events identified for LHF and SHF in the Alps, the 2014 event is consistent with our temperature results, since it recorded the lowest irrigation cooling throughout the entire study period. However, in 2017, although we can observe a clear cooling effect, other years demonstrated even greater cooling than what was recorded in 2017. Regarding the heat wave event in 2018 in Germany, temperatures in Mid-Europe show only a decrease at the beginning of the irrigation season. Nevertheless, we expected a higher impact since the interactions between the land and atmosphere show distinct behaviors in wet versus dry years (Qian et al., 2013). Therefore, in the next sections, we examine daily means to see a more detailed impact.

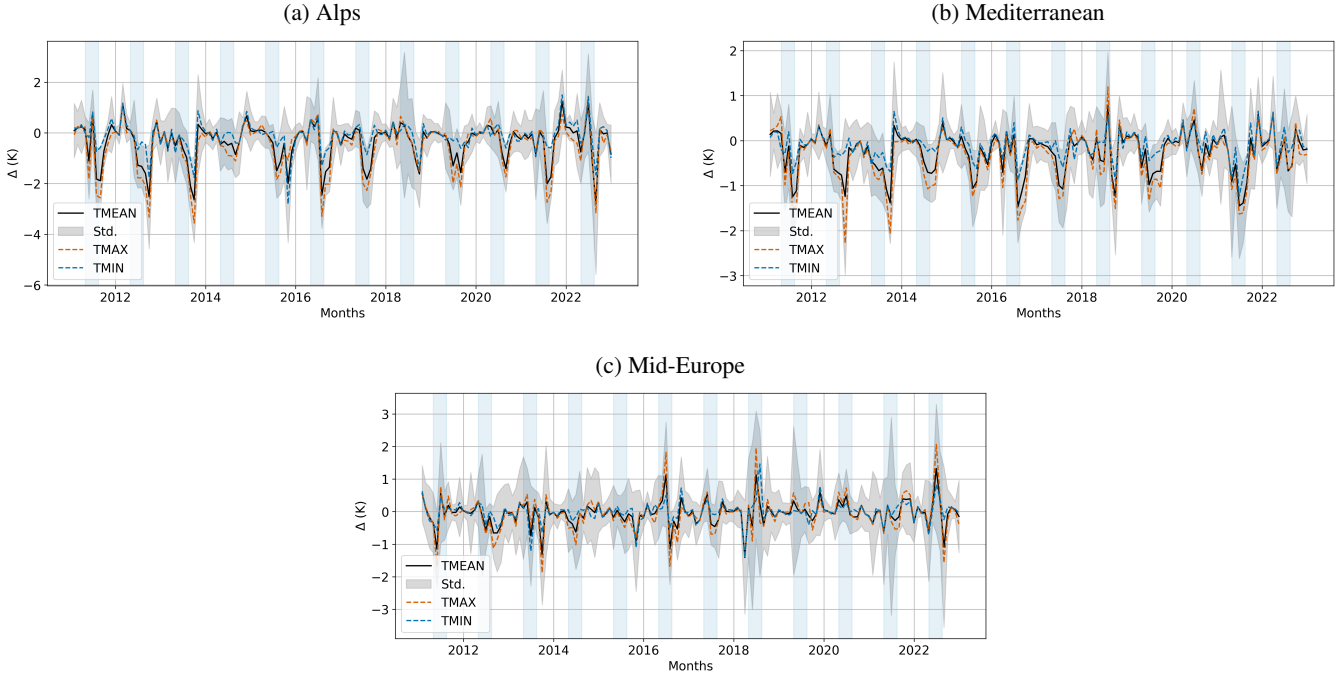

Figure 9. Timseries of monthly mean differences per prudence region, irrigation minus control, for temperature 2-m (mean, maximum and minimum). Blue shading indicates the irrigation period, from May to August of each year.

4.3 Irrigation effects on Weather extremes

Here, we focus on two heat wave (HW) events in Europe, one in the Alps region and another one in Mid-Europe. We added the ICON-DREAM reanalysis as a reference dataset for daily soil moisture (sm) and temperature comparisons, which are averaged over irrigated areas in the study regions.

https://doi.org/10.5194/egusphere-2026-3354
Preprint. Discussion started: 10 July 2026

4.3.1 Heat wave in southern Europe

The HW event in southern Europe reached its peak during the period August 3–5, 2017. This is visible in the lower sm values depicted in Figure 10a for this particular period. The figure also indicates that the ICON-DREAM dataset reached its lowest sm on August 5th, approximately 8.4 kg m^{-2}. The irrigation experiment attained the minimum sm in August 4th and, due to the irrigation event on August 5th, sm increased on this date already. In contrast, sm in the control run does not fluctuate as much as ICON-DREAM or the irrigation experiment. The sm fluctuations over time in ICON-DREAM might be related to the soil moisture analysis, which is done daily at 00UTC. In general, sm values from the irrigation run are much closer to the reanalysis than the control run, showing that the lack of irrigation in the Alps in a free simulation increases the sm biases. The 2017 HW is also visible in temperature values since Tmax_2m reached values higher than 305 K (∼31.85 °C) for all datasets during the HW period (Figure 10c). During this HW, the differences between the control and irrigation run for Tmax_2m and T2m are comparable with the differences visible just after the irrigation event on August 5th. After the HW peak on August 4th, the control and ICON-DREAM temperatures start decreasing, whereas the irrigation experiment begins to decrease one day after (August 5th). Asmus et al. (2023) also found a Tmax_2m reduction during this HW, -1.5 K for the 3rd and 4th of August in their irrigated simulation. Differently from our study, they used the REMO2020-iMOVE model, a different parameterization approach and an irrigation period from April to July. Since we irrigated on July 24th, the Tmax_2m and T2m in our irrigation experiment reduced more than -2 K in both cases for the same dates (August 3rd-4th) and our temperature reduction reached more than -3 K once the irrigation event took place (August 5th).

To corroborate the results during the HW period and the irrigation effect, we also show the diurnal cycle of the energy fluxes and the Bowen ratio for two periods: diurnal average over 4 days before irrigation and 4 days after irrigation (Figures 11). During the HW (4 days before irrigation) the control run characterizes by being highly dominated by SHF, since the Bowen ratio reaches values of 6.64 at 12 UTC while the irrigation experiment reaches only 1.62. So, eventhough an irrigation event occured 12 days before, its effect is still present during the HW. During the period August 5–8, the irrigation effect in more evident, since the energy loses are dominated by LHF, being the Bowen ratio 0.96. Miralles et al. (2019) mentioned that alterations to land, including irrigation, influence the regional land feedback mechanisms during periods of extreme heat and dryness, and our results confirm this for the HW in the Alps region in 2017.

https://doi.org/10.5194/egusphere-2026-3354
Preprint. Discussion started: 10 July 2026

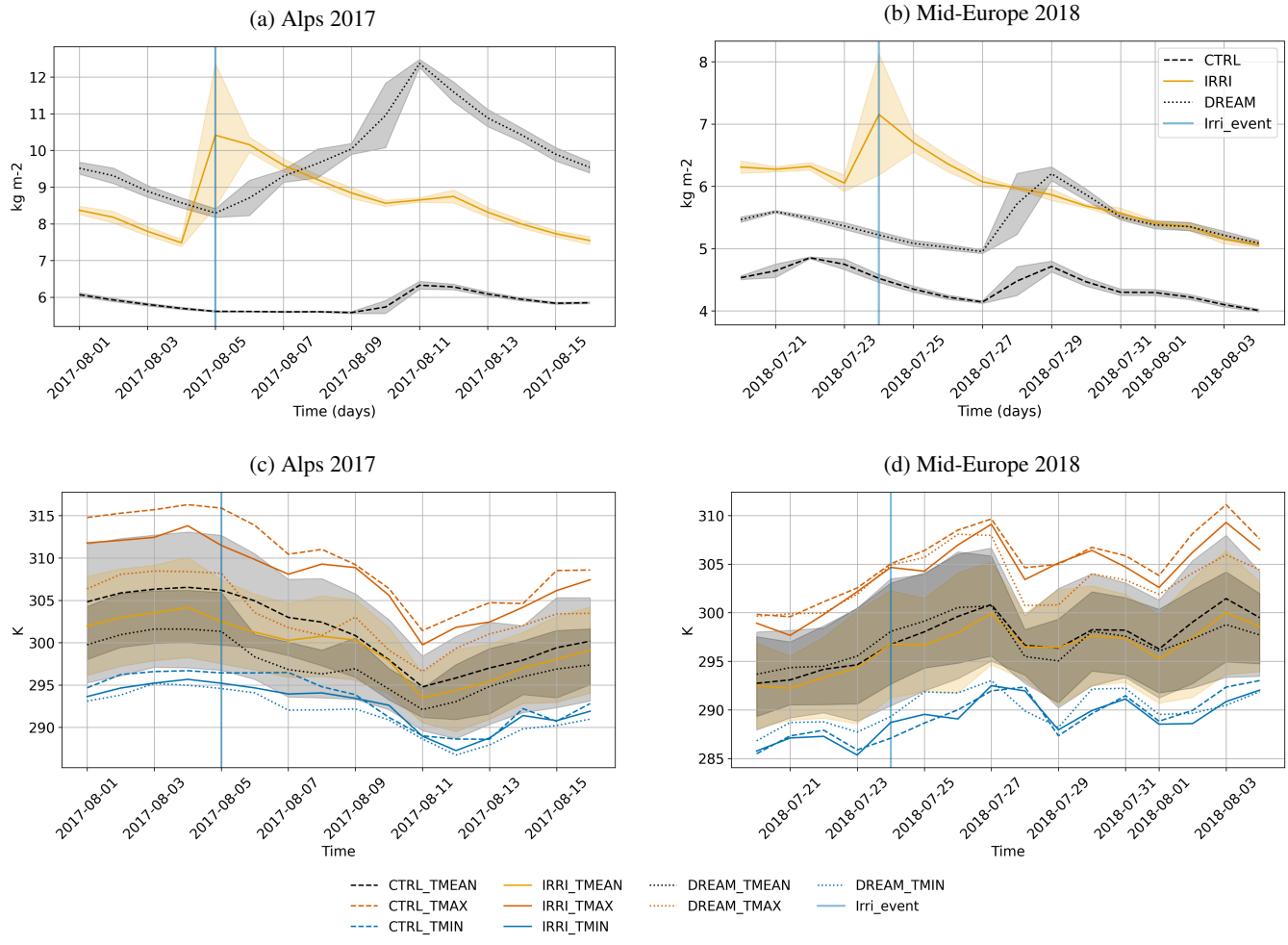

Figure 10. Irrigation effect on soil moisture (0-9 cm) and Temperature 2-m (mean, maximum and minimum) in different heat wave events. The vertical line represents the date of the irrigation event.

4.3.2 Heat wave in central Europe

The HW in central Europe started on July 23rd, 2018 (Rousi et al., 2023), which is one day before an irrigation event in our experiment. Therefore, sm in the irrigation experiment increases on July 24th, while the control and ICON-DREAM sm started reducing even before the HW started (Figure 10b). This early sm reduction aligns with the fact that, alongside the heatwave of 2018, central Europe simultaneously faced a pronounced drought (McNamara et al., 2024; Moravec et al., 2021). During the first 4 HW days, the differences between the control and irrigation experiment are clear for Tmax_2m, reducing around 1 K in the irrigation experiment. On July 27th, HW peak, this difference reduces and fluctuates over time until August 29th (Figure 10d), one day before the HW peak in Germany. However, the differences between the control and irrigation experiment

https://doi.org/10.5194/egusphere-2026-3354
Preprint. Discussion started: 10 July 2026

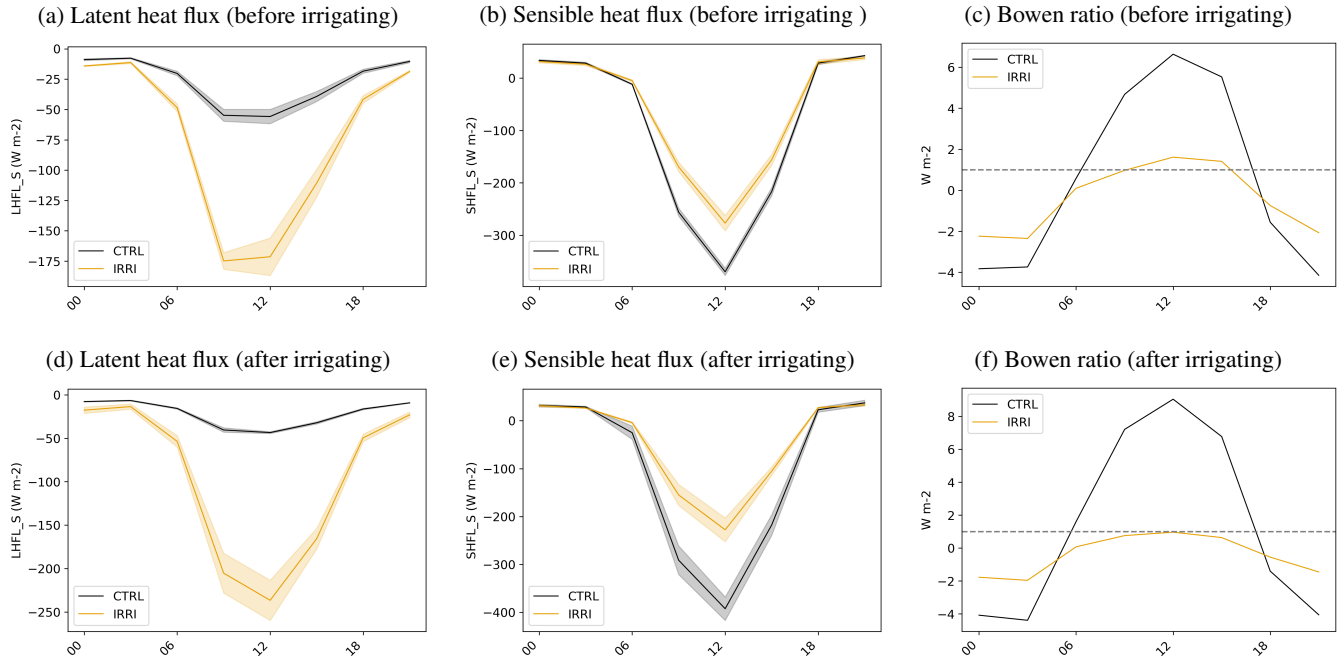

Figure 11. Diurnal cycle representation before and after an irrigation event during a heat wave in the Alps. (a), (b) and (c) average across four days from August 1st to 4th (before irrigation event). (d), (e) and (f) average across four days from August 5th to 8th (after irrigation event).

are visible again during this HW peak, July 30th – August 2nd. These examples further validate the findings presented in Sect. 4.2.2, demonstrating that exceptional events characterized by low sm values, in conjunction with elevated temperatures, transition the evaporative regime from energy-limited to moisture-limited as also found in Rousi et al. (2023).

We verified this regime change showing the diurnal cycle during the period before (July 20th to 23rd) and after (July 24th to 27th) irrigation (Figure 12). Generally, the difference between the irrigation and the control run over Mid-Europe for LHF and SHF is minimal compared with results over the Alps or the Mediterranean. However, during the 2018 HW before the irrigation event, LHF in the irrigation experiment already increased on average 42.15% while SHF decreased on average 17.10% in comparison with the control run. Moreover, in the days before the irrigation event, the average Bowen ratio for the control experiment is above 1, reaching 2.65 at 12UTC, which usually reaches values below one even in summer during normal years. The HW also allows us to show the irrigation effect in Mid -Europe, since the Bowen ratio for the irrigation experiment reaches only 1.50 at 12UTC. After the irrigation event on July 24th, the difference between the irrigation and control experiments increases on average to 77.66% and 27.39% for LHF and SHF respectively. Since the HW continues until August 9th, SHF continues dominating the energy loss, mainly for the control run. This is reflected in the Bowen ratio, which reaches 3.33 at 12 UTC in the control run, compared to 1.39 in the irrigation experiment. The lower Bowen ratio in the irrigation experiment indicates a shift toward latent heat flux, representing a larger reduction in SHF compared with the days

https://doi.org/10.5194/egusphere-2026-3354
Preprint. Discussion started: 10 July 2026

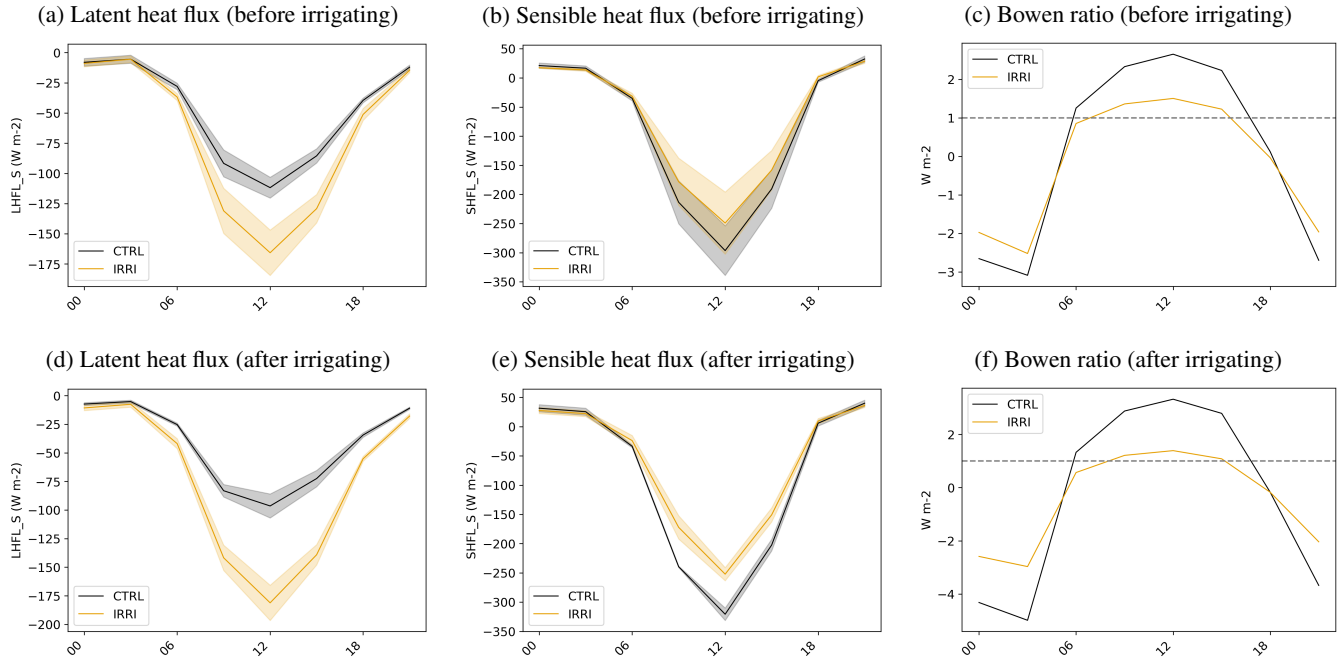

Figure 12. Diurnal cycle representation before and after an irrigation event during a heat wave in Mid-Europe. (a), (b) and (c) average across four days from July 20th to 23rd (before irrigation event). (d), (e) and (f) average across four days from July 24th to 27th (after irrigation event).

before irrigation event. Our results in central Europe coincide with the findings of Liu et al. (2020), the 2018 HW intensifies the soil moisture-temperature coupling, allowing our irrigation experiment to influence T2m changes.

5 Conclusions

The integration of irrigation into coupled Earth System Models has facilitated the identification of its interactions with different components of the Earth system (McDermid et al., 2023). In this study, we quantified the long-term impact of irrigation on surface and atmospheric variables over Europe using convection-permitting simulations, allowing us to investigate its multi-year effects on this region. To our knowledge, this is among the first studies to assess irrigation impacts over the whole European continent at convection-permitting scales over a multi-year timeframe. This long-term simulations also allowed the assessment of the irrigation effect on weather extremes across different years and enhanced the visibility of irrigation on model performance through time. Some regional (Asmus et al., 2023) and local (Valmassoi et al., 2020b) studies in Europe have investigated the irrigation impact in case studies that included a simulation period of one crop growing season. They found the characteristic cooling effect on 2-m temperature in irrigated areas and a bias reduction of this variable when comparing with observations.

https://doi.org/10.5194/egusphere-2026-3354
Preprint. Discussion started: 10 July 2026

Our research found that in the EURO-CORDEX domain the magnitude of the irrigation impact is limited by the irrigated region and the year. Also land-atmosphere coupling is crucial to determine the irrigation effects, as these impacts are less evident under wet conditions and more pronounced under dry conditions. For instance, the unusual cold and wet summer of 2014 in southern Europe (Ratna et al., 2017) lead to the lowest irrigation cooling throughout our entire study period in the Alps. While the heat wave of 2018 in Central Europe intensified the soil moisture-temperature coupling Liu et al. (2020), allowing our irrigation experiment to influence the energy fluxes and temperature changes.

Our findings align with previous irrigation studies conducted in other regions that similarly identified the link between weak land–atmosphere coupling (Lower Mississippi River Basin and eastern China) and the negligible impact of irrigation (McDermid et al., 2023; Chen and Dirmeyer, 2019). However, regions that are normally under the energy-limited evaporative regime, during prolonged droughts and heat waves, might transition to the moisture-limited regime (Rousi et al., 2023). Under these circumstances, not only the irrigation requerements increase (McNamara et al., 2024) but also due to climate change these scenarios might become more frequent. Consequently, it is essential to incorporate irrigation in climate modeling across all regions, taking into account the characteristics of each region.

The 2-m temperature evaluation in model performance in four subregions indicates that the Alps and Mediterranean benefit from including irrigation in the ICON model with the current settings, while the biases in the Iberian Peninsula increased during the whole irrigated season. The overall evaluation in Mid-Europe shows a bias reduction only significant for July and August. The bias deterioration might be linked with some of the limitations of our study. For instance, our irrigation scheduling starts at 5UTC, however, night irrigation is common in the Ebro basin (Lunel et al., 2024; Altés et al., 2023). In the case of Mid-Europe, the number of irrigation events and the irrigation amount is usually lower than what we applied. As a result, our parameterization requires more flexibility in the specification of the irrigation settings, considering regional characteristics. Additionally, we incorporated irrigation water sourced externally to the system, therefore, it was not subtracted from other water reserves to maintain the water balance (Zhou et al., 2020). Furthermore, we incorporated a constant root depth in the parameterization, despite the fact that this variable can differ significantly among crops, their growth stage and even the modeler choice. For instance, Marcella and Eltahir (2014) also considers a constant root zone, but with a depth of 1 m. While Wu et al. (2018) works with the first and second soil layers, 0.4 m in total. A more effective approach may involve considering the root depth in relation to crop type, however, our LSM currently lacks this crop representation.

Consequently, future work should include the consideration of different crop types in the LSM since the irrigation impact is different per crop type. For example, a the case study based on the LIAISE field campaign, Lunel et al. (2025) reported a different specific humidity performance across crop types. Unlike us, they studied the diurnal performance of the irrigation simulations and found that while specific humidity is overestimated in a corn field, irrigation simulations in alfalfa fields improve this variable throughout the day. Also, the evaluation of other variables such as wind speed, direction and the ET should be considered, similar to the work of Lunel et al. (2024). Moreover, when investigating the irrigation effect on extreme events, relative humidity should be included since irrigation can intensify moist heat stress (McDermid et al., 2023). Finally, Lawston-Parker et al. (2023) suggested the use of high-resolution irrigation datasets that resolve the extensive irrigation boundaries and reflect the variability of irrigation practices within regions. Currently, the new dataset European Crop-specific IRrigated Area

https://doi.org/10.5194/egusphere-2026-3354
Preprint. Discussion started: 10 July 2026

(ECIRA) is available at 1 km resolution, being crop-specific and available for each year from 2010 to 2020 (Zhu et al., 2025). Our simulations at 3 km resolution might benefit from the use of this high resolution irrigation map.

Code and data availability.
- The ICON model is available at https://gitlab.dkrz.de/icon/icon-model
- The irrigation parameterization to be implemented in ICON-NWP is available at https://doi.org/10.60507/FK2/YIGGOC
- The irrigation and control monthly data is available at https://doi.org/10.5281/zenodo.20606101
- Initial and lateral boundary conditions to run ICON-nwp were obtained from ICON-DREAM and are available at doi:10.5676/dwd/icon-dream_v1

Appendix A

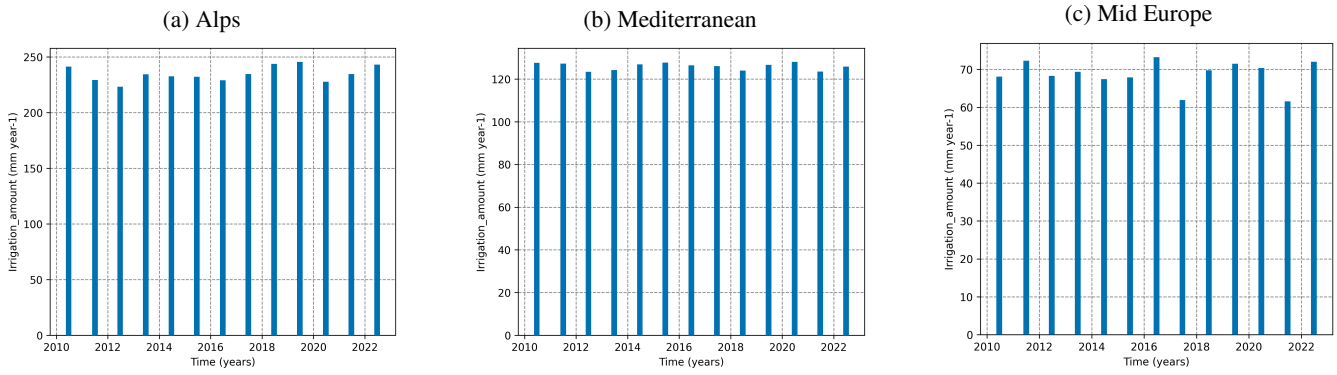

Figure A1. Annual mean irrigation amount per prudence region in mm year^{-1}.

https://doi.org/10.5194/egusphere-2026-3354
Preprint. Discussion started: 10 July 2026

Region	Exp.	May	June	July	August	September
Alps	CTRL	-0.018	-0.034	-0.081	-0.104	-0.067
	IRRI	-0.016	-0.033	-0.064	-0.078	-0.053
	ABS	-0.001*	-0.001*	-0.017*	-0.025*	-0.013*
Mediterranean	CTRL	-0.015	-0.036	-0.067	-0.068	-0.032
	IRRI	-0.009	-0.023	-0.045	-0.047	-0.021
	ABS	-0.007*	-0.013*	-0.022*	-0.021*	-0.011*
Iberian P.	CTRL	0.006	0.001	-0.011	-0.012	0.002
	IRRI	0.013	0.012	0.004	0.002	0.007
	ABS	0.007*	0.011*	-0.006*	-0.010*	0.005*
Mid-Europe	CTRL	0.010	-0.012	-0.037	-0.046	-0.038
	IRRI	0.013	-0.019	-0.034	-0.039	-0.031
	ABS	0.003*	0.006*	-0.003	-0.007*	-0.006*

Table A1. Control and irrigation biases from May to September considering all observations present in each Prudence region for Relative Humidity. ABS is the absolute difference between IRRI and CTRL.

(*) Statistically significant change in the bias due to irrigation (5% significance level on two-sided Wilcoxon signed rank test on multi-annual data).

https://doi.org/10.5194/egusphere-2026-3354
Preprint. Discussion started: 10 July 2026

Region	Exp.	May	June	July	August	September
Alps	CTRL	-0.46	0.43	2.23	2.94	1.17
	IRRI	-0.71	-0.01	0.70	1.02	0.16
	ABS	0.25*	-0.42*	-1.53*	-1.92*	-1.02*
Mediterranean	CTRL	0.01	0.73	1.72	1.45	1.01
	IRRI	-0.46	0.01	0.53	0.28	0.44
	ABS	0.45*	-0.72*	-1.19*	-1.17*	-0.57*
Iberian P.	CTRL	-0.64	-0.28	-0.04	-0.19	-0.29
	IRRI	-1.04	-0.96	-0.97	-1.01	-0.79
	ABS	0.40*	0.68*	0.93*	0.82*	0.50*
Mid-Europe	CTRL	-0.73	-0.01	0.53	0.69	0.24
	IRRI	-0.86	0.06	0.42	0.35	0.14
	ABS	0.13	0.05	-0.10*	-0.35*	-0.10

Table A2. Control and irrigation biases from May to September considering all observations present in each Prudence region (irrigated areas) for 2-m Temperature. ABS is the absolute difference between IRRI and CTRL.

(*) Statistically significant change in the bias due to irrigation (5% significance level on two-sided Wilcoxon signed rank test on multi-annual data).

https://doi.org/10.5194/egusphere-2026-3354
Preprint. Discussion started: 10 July 2026

Region	Exp.	May	June	July	August	September
Alps	CTRL	-0.05	-0.11	-0.20	-0.23	-0.13
	IRRI	-0.03	-0.06	-0.12	-0.13	-0.09
	ABS	-0.02*	-0.04*	-0.08*	-0.10*	-0.04*
Mediterranean	CTRL	-0.03	-0.07	-0.13	-0.14	-0.09
	IRRI	-0.01	-0.03	-0.07	-0.07	-0.06
	ABS	-0.03*	-0.04*	-0.06*	-0.06*	-0.04*
Iberian P.	CTRL	0.00	0.00	-0.03	-0.03	-0.01
	IRRI	0.03	0.04	0.02	0.02	0.01
	ABS	0.03*	0.03*	-0.01*	-0.02*	0.00*
Mid-Europe	CTRL	0.01	-0.02	-0.06	-0.07	-0.05
	IRRI	0.02	-0.02	-0.04	-0.05	-0.04
	ABS	0.01*	0.00	-0.02*	-0.02*	-0.01*

Table A3. Control and irrigation biases from May to September considering all observations present in each Prudence region (irrigated areas) for Relative humidity. ABS is the absolute difference between IRRI and CTRL.
(*) Statistically significant change in the bias due to irrigation (5% significance level on two-sided Wilcoxon signed rank test on multi-annual data).

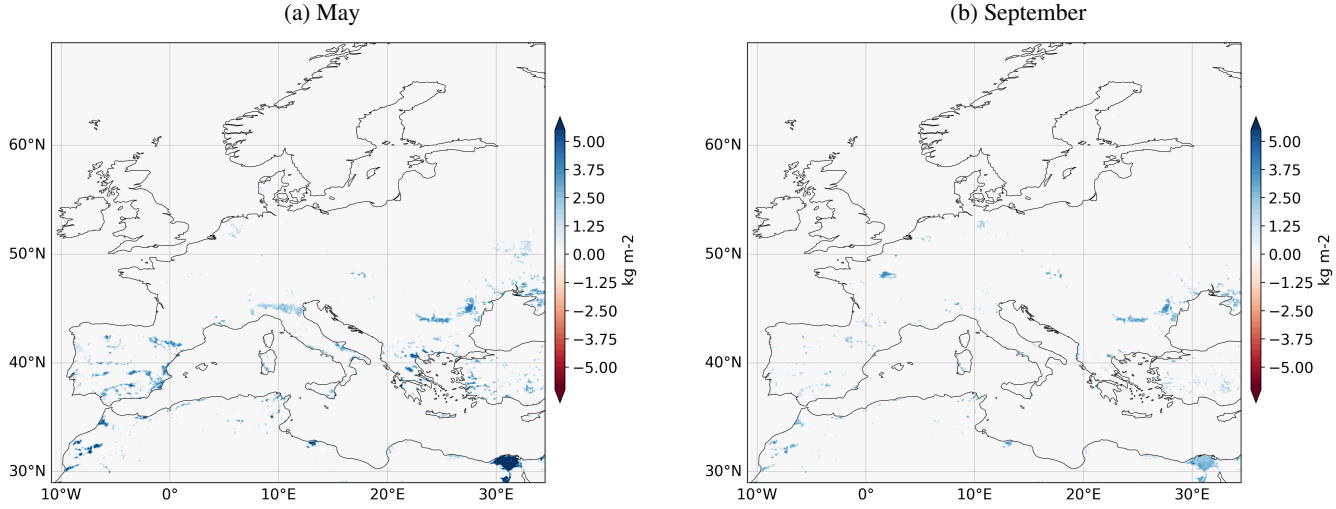

Figure A2. Monthly soil moisture (0 - 9 cm) mean differences for May and September (2011-2022).

https://doi.org/10.5194/egusphere-2026-3354
Preprint. Discussion started: 10 July 2026

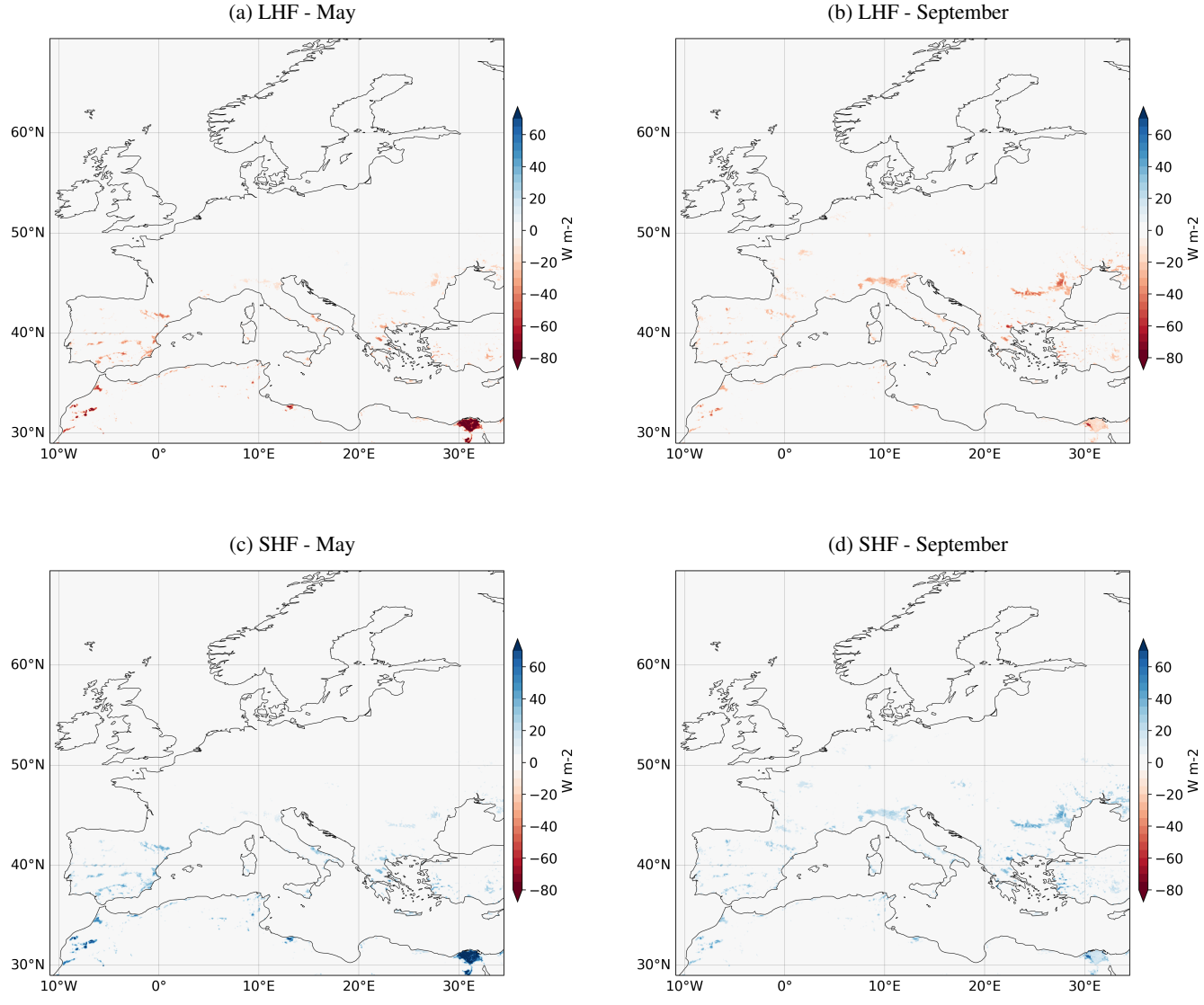

Figure A3. Monthly energy fluxes mean differences for May and September (2011-2022).

https://doi.org/10.5194/egusphere-2026-3354
Preprint. Discussion started: 10 July 2026

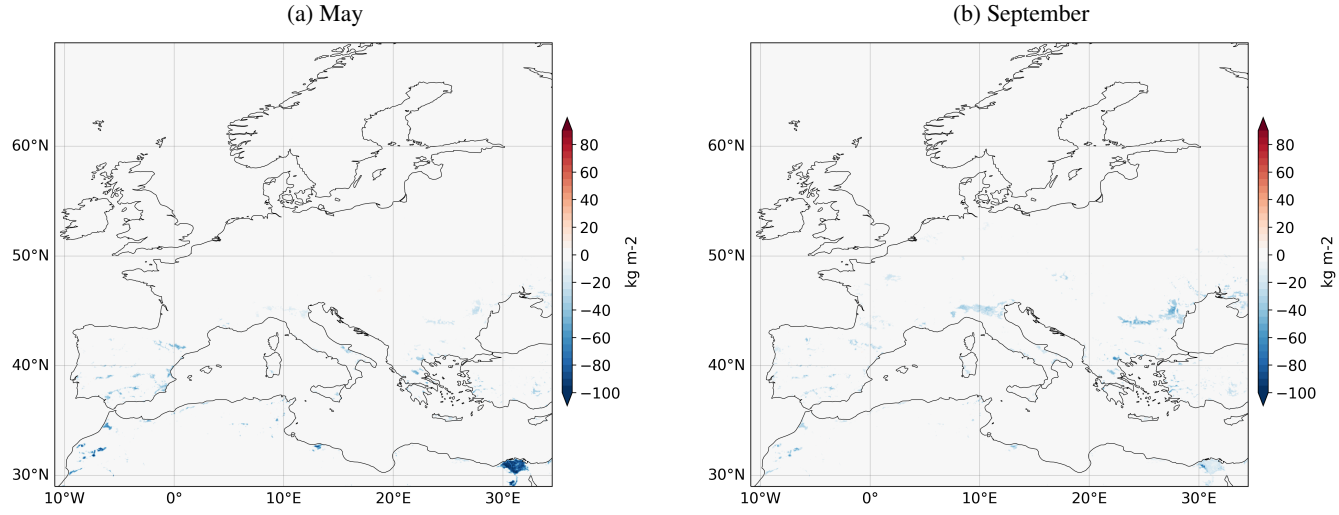

Figure A4. Monthly evapotranspiration mean differences for May and September (2011-2022).

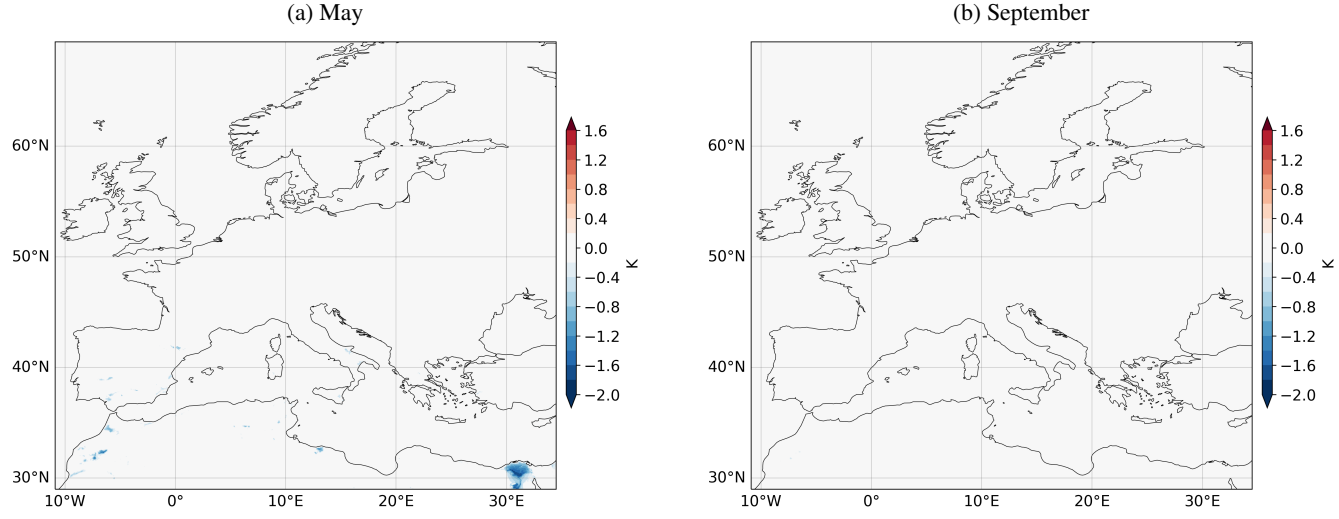

Figure A5. Monthly temperature 2 m mean differences for May and September (2011-2022).

https://doi.org/10.5194/egusphere-2026-3354
Preprint. Discussion started: 10 July 2026

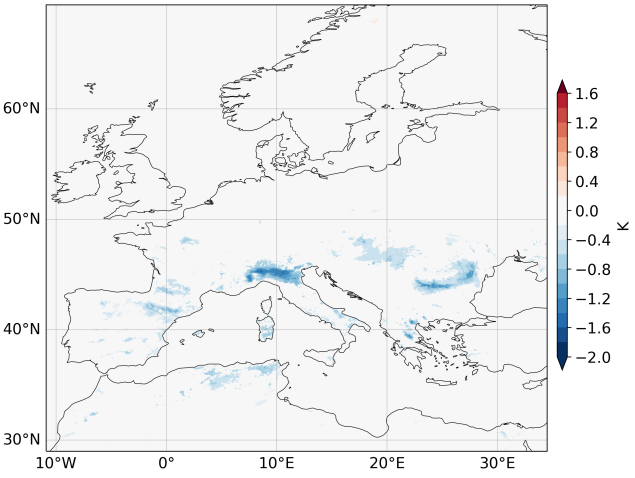

Figure A6. Monthly temperature 2 m mean differences for September with t-test (2011-2022).

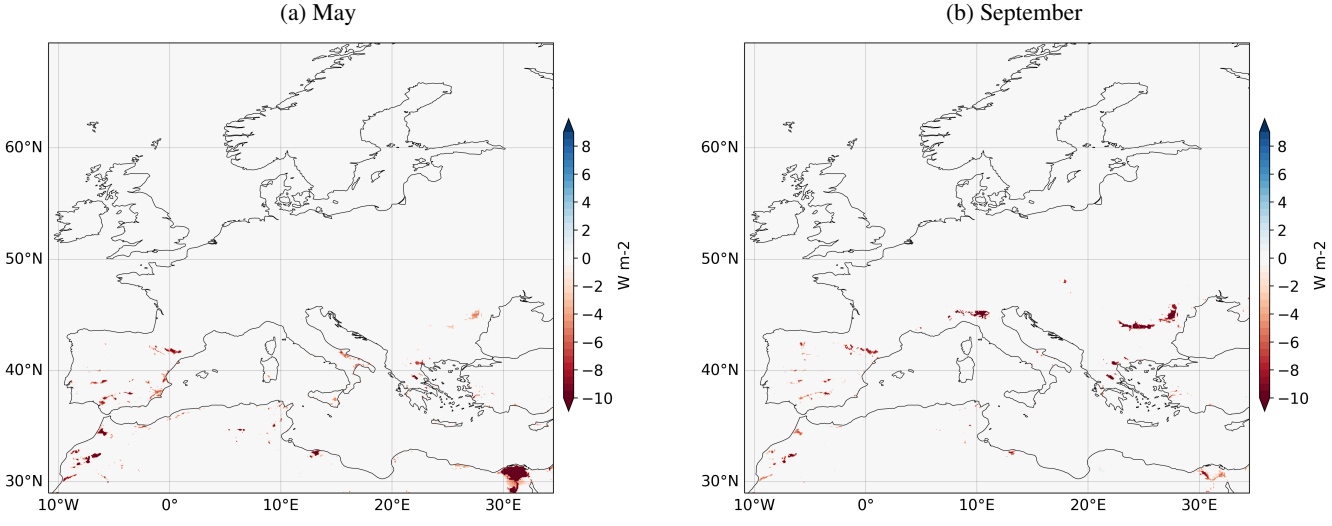

Figure A7. Monthly upward long wave radiation differences for May and September (2011-2022).

https://doi.org/10.5194/egusphere-2026-3354
Preprint. Discussion started: 10 July 2026

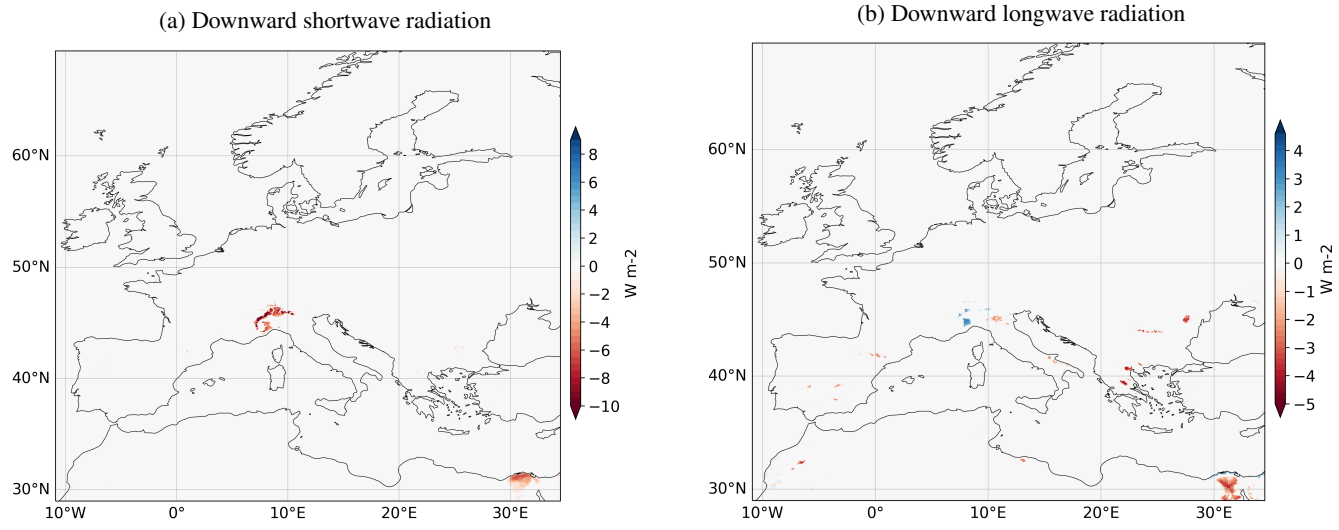

Figure A8. Downward shortwave and longwave radiation differences for JJA (2011-2022).

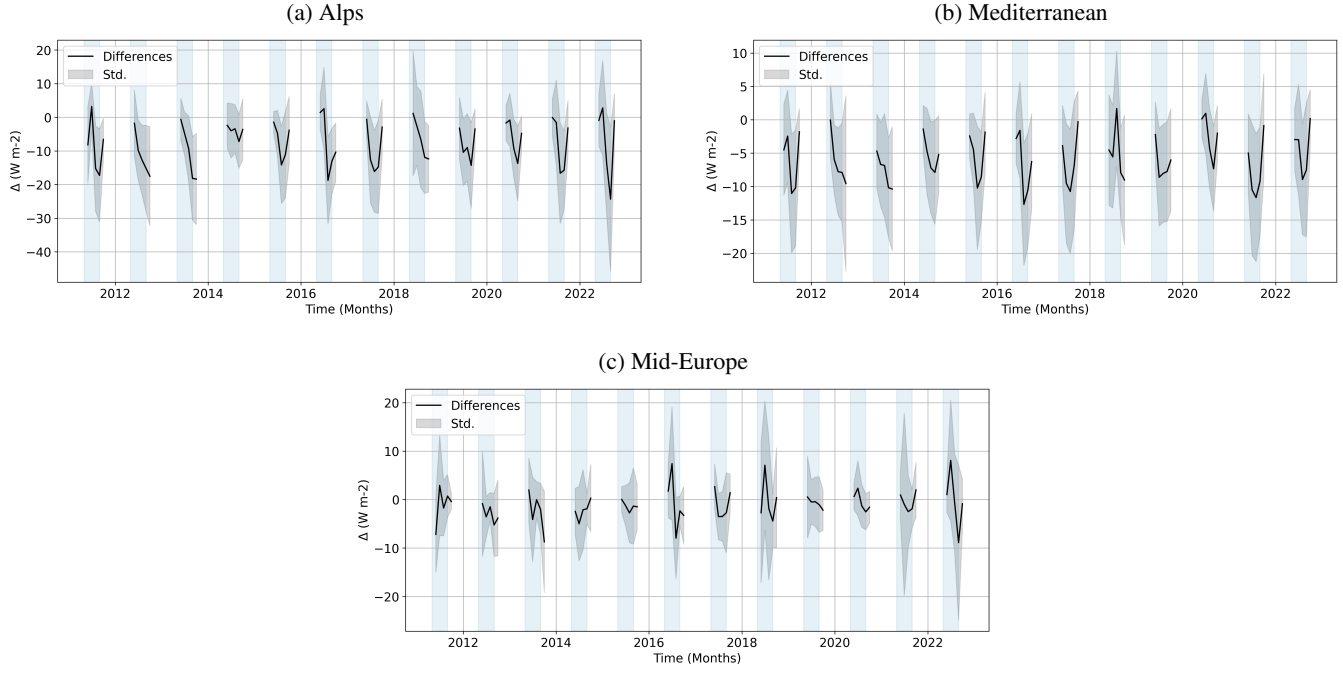

Figure A9. Timseries of monthly mean differences per prudence region, irrigation - control for upward longwave radiation for May, June, July, August and September. Blue shading indicates the irrigation period, from May to August of each year.

https://doi.org/10.5194/egusphere-2026-3354
Preprint. Discussion started: 10 July 2026

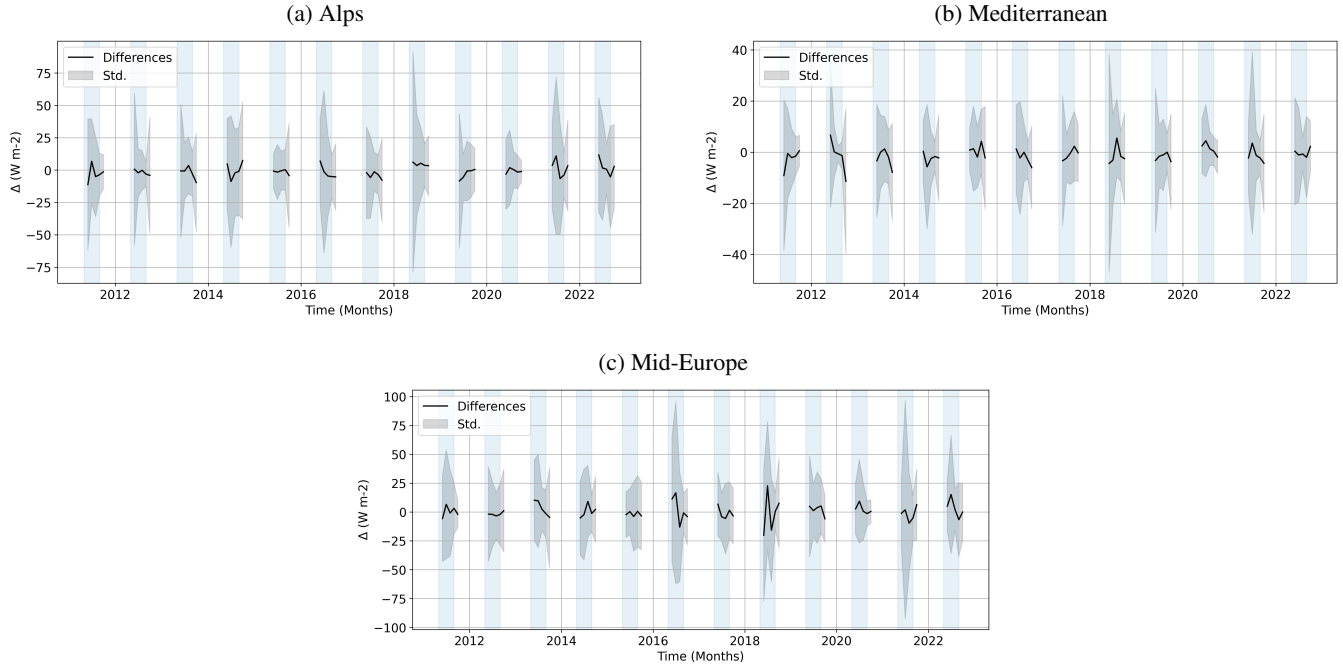

Figure A10. Timseries of monthly mean differences per prudence region, irrigation - control for net radiation for May, June, July, August and September. Blue shading indicates the irrigation period, from May to August of each year.

https://doi.org/10.5194/egusphere-2026-3354
Preprint. Discussion started: 10 July 2026

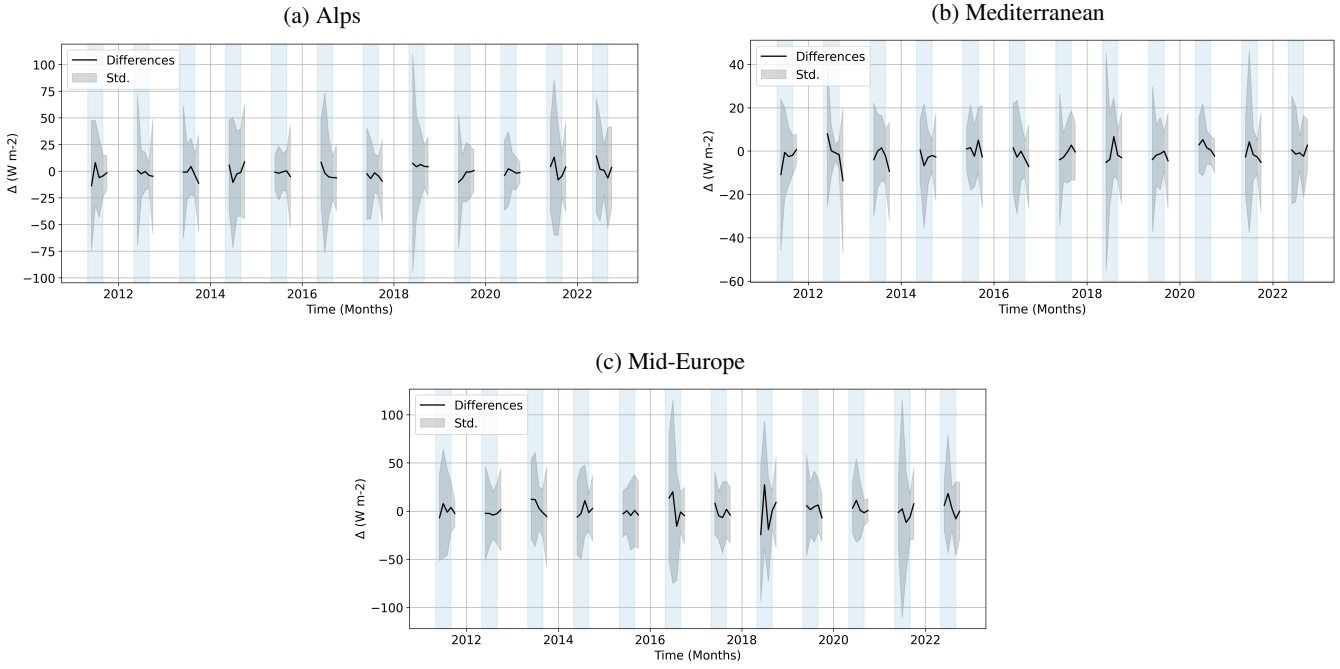

Figure A11. Timseries of monthly mean differences per prudence region, irrigation - control for downward shortwave radiation for May, June, July, August and September. Blue shading indicates the irrigation period, from May to August of each year.

Author contributions. Roque, J.L. contributed on the following: Conceptualization, Investigation, Writing - original draft, Methodology, Validation, Visualization, Software, Formal analysis. Valmassoi, A. contributed on the following:Conceptualization, Investigation, Funding acquisition, Methodology, Writing - review and editing, Project administration, Software, Supervision, Resources.

Competing interests. The authors declare that they have no conflict of interest.

Acknowledgements. We express our gratitude to Prof. Stefan Siebert for his invaluable insights on irrigation, which have been key in defining the irrigation settings in the parameterization for this study.

We thankfully acknowledge the Deutsche Wetterdienst (DWD - German Weather Service) for providing computing resources in the operational High Performance Computing system. Additionally, we extend our appreciation to Daniel Rieger for his assistance in addressing all our inquiries regarding ICON-nwp and ICON tools.

This publication was supported by the Open Access Publication Fund of the University of Bonn.

https://doi.org/10.5194/egusphere-2026-3354
Preprint. Discussion started: 10 July 2026

Financial support

The authors acknowledge funding by the Deutsche Forschungsgemeinschaft (DFG, German Research Foundation) in the Collaborative Research Centre "DETECT" SFB 1502/1-2022 Project No. 450058266.

https://doi.org/10.5194/egusphere-2026-3354
Preprint. Discussion started: 10 July 2026

References

Allen, R., Pereira, L., Raes, D., and Smith, M.: Crop Evapotranspiration: Guidelines for Computing Crop Requirements, Tech. rep., FAO, https://www.fao.org/4/x0490e/x0490e00.htm#Contents, 1998.

Altés, V., Bellvert, J., Pascual, M., and Villar, J. M.: Understanding Drainage Dynamics and Irrigation Management in a Semi-Arid Mediterranean Basin, Water (Switzerland), 15, https://doi.org/10.3390/w15010016, 2023.

Asmus, C., Hoffmann, P., Pietikäinen, J. P., Böhner, J., and Rechid, D.: Modeling and evaluating the effects of irrigation on land-atmosphere interaction in southwestern Europe with the regional climate model REMO2020-iMOVE using a newly developed parameterization, Geoscientific Model Development, 16, 7311–7337, https://doi.org/10.5194/gmd-16-7311-2023, 2023.

Azar, R., Villa, P., Stroppiana, D., Crema, A., Boschetti, M., and Brivio, P. A.: Assessing in-season crop classification performance using satellite data: A test case in Northern Italy, European Journal of Remote Sensing, 49, 361–380, https://doi.org/10.5721/EuJRS20164920, 2016.

Benjamini, Y. and Hochberg, Y.: Controlling the False Discovery Rate: A Practical and Powerful Approach to Multiple Testing, Journal of the Royal Statistical Society: Series B (Methodological), 57, 289–300, https://doi.org/https://doi.org/10.1111/j.2517-6161.1995.tb02031.x, 1995.

Benson, D. O. and Dirmeyer, P. A.: Characterizing the relationship between temperature and soil moisture extremes and their role in the exacerbation of heat waves over the contiguous United States, Journal of Climate, 34, 2175–2187, https://doi.org/10.1175/JCLI-D-20-0440.1, 2021.

Bos, M. G.: Using the depleted fraction to manage the groundwater table in irrigated areas, Irrigation and Drainage Systems, 18, 201–209, 2004.

Brekel, J., Thorp, K. R., DeJonge, K. C., and Trout, T. J.: Version 1.1.0—pyfao56: FAO-56 evapotranspiration in Python, SoftwareX, 22, 101 336, https://doi.org/https://doi.org/10.1016/j.softx.2023.101336, 2023.

Brooke, J. K., Best, M. J., Lock, A. P., Osborne, S. R., Price, J., Cuxart, J., Boone, A., Canut-Rocafort, G., Hartogensis, O. K., and Roy, A.: Irrigation contrasts through the morning transition, Quarterly Journal of the Royal Meteorological Society, 150, 170–194, https://doi.org/10.1002/qj.4590, 2024.

Chen, L. and Dirmeyer, P. A.: Global observed and modelled impacts of irrigation on surface temperature, International Journal of Climatology, 39, 2587–2600, https://doi.org/10.1002/joc.5973, 2019.

Cook, B. I., Shukla, S. P., Puma, M. J., and Nazarenko, L. S.: Irrigation as an historical climate forcing, Climate Dynamics, 44, 1715–1730, https://doi.org/10.1007/s00382-014-2204-7, 2015.

de Vrese, P. and Hagemann, S.: Uncertainties in modelling the climate impact of irrigation, Climate Dynamics, 51, 2023–2038, https://doi.org/10.1007/s00382-017-3996-z, 2018.

Deb, P., Moradkhani, H., Han, X., Abbaszadeh, P., and Xu, L.: Assessing irrigation mitigating drought impacts on crop yields with an integrated modeling framework, Journal of Hydrology, 609, https://doi.org/10.1016/j.jhydrol.2022.127760, 2022.

Eekhout, J. P., Delsman, I., Baartman, J. E., van Eupen, M., van Haren, C., Contreras, S., Martínez-López, J., and de Vente, J.: How future changes in irrigation water supply and demand affect water security in a Mediterranean catchment, Agricultural Water Management, 297, https://doi.org/10.1016/j.agwat.2024.108818, 2024.

Fan, Y., Yang, Z., Lo, M.-H., Hur, J., and Im, E.-S.: Deciphering the capricious precipitation response: irrigation impact in the North China Plain, npj Climate and Atmospheric Science, 8, 211, https://doi.org/10.1038/s41612-025-01063-3, 2025.

https://doi.org/10.5194/egusphere-2026-3354
Preprint. Discussion started: 10 July 2026

Guillod, B. P., Davin, E. L., Kündig, C., Smiatek, G., and Seneviratne, S. I.: Impact of soil map specifications for European climate simulations, Climate Dynamics, 40, 123–141, https://doi.org/10.1007/s00382-012-1395-z, 2013.

Hoy, A., Hänsel, S., and Maugeri, M.: An endless summer: 2018 heat episodes in Europe in the context of secular temperature variability and change, International Journal of Climatology, 40, 6315–6336, https://doi.org/10.1002/joc.6582, 2020.

Ionita, M., Dima, M., Nagavciuc, V., Scholz, P., and Lohmann, G.: Past megadroughts in central Europe were longer, more severe and less warm than modern droughts, Communications Earth and Environment, 2, https://doi.org/10.1038/s43247-021-00130-w, 2021.

JRC.D.5: Crop Calendar 2015: Unit 05 – Food Security, Tech. rep., Food Security Unit, Joint Research Centre (JRC.D.5), Directorate D – Sustainable Resources, https://agri4cast.jrc.ec.europa.eu/DataPortal/Index.aspx?o=d, 2015.

Kew, S. F., Philip, S. Y., van Oldenborgh, G. J., van der Schrier, G., Otto, F. E. L., and Vautard, R.: The Exceptional Summer Heat Wave in Southern Europe 2017, Bulletin of the American Meteorological Society, 100, 49–53, 2019.

Kim, J. H., Nam, S. H., Kim, M. K., Serrano-Notivoli, R., and Tejedor, E.: The 2022 record-high heat waves over southwestern Europe and their underlying mechanism, Weather and Climate Extremes, 46, https://doi.org/10.1016/j.wace.2024.100729, 2024.

Koster, R. D., Suarez, M. J., and Heiser, M.: American Meteorological Society Variance and Predictability of Precipitation at Seasonal-to-Interannual Timescales, Source: Journal of Hydrometeorology, 1, 26–46, https://doi.org/10.2307/24909280, 2000.

Lawston-Parker, P., Santanello, J. A., and Chaney, N. W.: Investigating the response of land-atmosphere interactions and feedbacks to spatial representation of irrigation in a coupled modeling framework, Hydrology and Earth System Sciences, 27, 2787–2805, https://doi.org/10.5194/hess-27-2787-2023, 2023.

Leng, G., Leung, L. R., and Huang, M.: Significant impacts of irrigation water sources and methods on modeling irrigation effects in the ACME Land Model, Journal of Advances in Modeling Earth Systems, 9, 1665–1683, https://doi.org/10.1002/2016MS000885, 2017.

Liu, X., He, B., Guo, L., Huang, L., and Chen, D.: Similarities and Differences in the Mechanisms Causing the European Summer Heatwaves in 2003, 2010, and 2018, Earth's Future, 8, https://doi.org/10.1029/2019EF001386, 2020.

Lo, M. H., Wey, H. W., Im, E. S., Tang, L. I., Anderson, R. G., Wu, R. J., Chien, R. Y., Wei, J., Kouchak, A. A., and Wada, Y.: Intense agricultural irrigation induced contrasting precipitation changes in Saudi Arabia, Environmental Research Letters, 16, https://doi.org/10.1088/1748-9326/ac002e, 2021.

Lobell, D., Bala, G., Mirin, A., Phillips, T., Maxwell, R., and Rotman, D.: Regional differences in the influence of irrigation on climate, Journal of Climate, 22, 2248–2255, https://doi.org/10.1175/2008JCLI2703.1, 2009.

Lorenz, R., Pitman, A. J., and Sisson, S. A.: Does Amazonian deforestation cause global effects; Can we be sure?, Journal of Geophysical Research, 121, 5567–5584, https://doi.org/10.1002/2015JD024357, 2016.

Lunel, T., Boone, A. A., and Moigne, P. L.: Irrigation strongly influences near-surface conditions and induces breeze circulation: Observational and model-based evidence, Quarterly Journal of the Royal Meteorological Society, 150, 2798–2819, https://doi.org/10.1002/qj.4736, 2024.

Lunel, T. R., Marti, B., Boone, A., and Moigne, P. L.: Systematic overestimation of evapotranspiration over irrigated areas by an offline land surface model, EGUsphere, https://doi.org/10.5194/egusphere-2024-3562, 2025.

Mangan, M. R., Hartogensis, O., Boone, A., Branch, O., Canut, G., Cuxart, J., de Boer, H. J., Page, M. L., Martínez-Villagrasa, D., Miró, J. R., Price, J., and de Arellano, J. V.-G.: The surface-boundary layer connection across spatial scales of irrigation-driven thermal heterogeneity: An integrated data and modeling study of the LIAISE field campaign, Agricultural and Forest Meteorology, 335, https://doi.org/10.1016/j.agrformet.2023.109452, 2023.

https://doi.org/10.5194/egusphere-2026-3354
Preprint. Discussion started: 10 July 2026

Marcella, M. P. and Eltahir, E. A.: Introducing an irrigation scheme to a regional climate model: A case study over West Africa, Journal of Climate, 27, 5708–5723, https://doi.org/10.1175/JCLI-D-13-00116.1, 2014.

McDermid, S., Nocco, M., Lawston-Parker, P., Keune, J., Pokhrel, Y., Jain, M., Jägermeyr, J., Brocca, L., Massari, C., Jones, A. D., Vahmani, P., Thiery, W., Yao, Y., Bell, A., Chen, L., Dorigo, W., Hanasaki, N., Jasechko, S., Lo, M. H., Mahmood, R., Mishra, V., Mueller, N. D., Niyogi, D., Rabin, S. S., Sloat, L., Wada, Y., Zappa, L., Chen, F., Cook, B. I., Kim, H., Lombardozzi, D., Polcher, J., Ryu, D., Santanello, J., Satoh, Y., Seneviratne, S., Singh, D., and Yokohata, T.: Irrigation in the Earth system, Nature Reviews Earth and Environment, 4, 435–453, https://doi.org/10.1038/s43017-023-00438-5, 2023.

McNamara, I., Flörke, M., Uschan, T., Baez-Villanueva, O. M., and Herrmann, F.: Estimates of irrigation requirements throughout Germany under varying climatic conditions, Agricultural Water Management, 291, https://doi.org/10.1016/j.agwat.2023.108641, 2024.

Miralles, D. G., Gentine, P., Seneviratne, S. I., and Teuling, A. J.: Land–atmospheric feedbacks during droughts and heatwaves: state of the science and current challenges, Annals of the New York Academy of Sciences, 1436, 19–35, https://doi.org/10.1111/nyas.13912, 2019.

Moravec, V., Markonis, Y., Rakovec, O., Svoboda, M., Trnka, M., Kumar, R., and Hanel, M.: Europe under multi-year droughts: How severe was the 2014–2018 drought period?, Environmental Research Letters, 16, https://doi.org/10.1088/1748-9326/abe828, 2021.

Nana, E., Corbari, C., and Bocchiola, D.: A model for crop yield and water footprint assessment: Study of maize in the Po valley, Agricultural Systems, 127, 139–149, https://doi.org/10.1016/j.agsy.2014.03.006, 2014.

Pop, C., Böhner, J., Hoffmann, P., Pietikäinen, J.-P., and Rechid, D.: The Role of Horizontal Resolution in Modeling Irrigation Effects With a Coupled Regional Climate Model System Up To Convection-Permitting Scale, Journal of Geophysical Research: Atmospheres, 130, e2024JD043 227, https://doi.org/https://doi.org/10.1029/2024JD043227, e2024JD043227 2024JD043227, 2025.

Qian, Y., Huang, M., Yang, B., and Berg, L. K.: A modeling study of irrigation effects on surface fluxes and land-air-cloud interactions in the southern great plains, Journal of Hydrometeorology, 14, 700–721, https://doi.org/10.1175/JHM-D-12-0134.1, 2013.

Qian, Y., Yang, Z., Feng, Z., Liu, Y., Gustafson, W. I., Berg, L. K., Huang, M., Yang, B., and Ma, H. Y.: Neglecting irrigation contributes to the simulated summertime warm-and-dry bias in the central United States, npj Climate and Atmospheric Science, 3, https://doi.org/10.1038/s41612-020-00135-w, 2020.

Ratna, S. B., Ratnam, J. V., Behera, S. K., Cherchi, A., Wang, W., and Yamagata, T.: The unusual wet summer (July) of 2014 in Southern Europe, Atmospheric Research, 189, 61–68, https://doi.org/10.1016/j.atmosres.2017.01.017, 2017.

Roque, J. L. and Valmassoi, A.: How do Irrigation Schemes shape the Irrigation Impact? A Sensitivity Test with the Operational ICON-NWP, ESS Open Archive preprint, https://doi.org/10.22541/essoar.176530330.04410565/v1, 2025.

Rousi, E., Fink, A. H., Andersen, L. S., Becker, F. N., Beobide-Arsuaga, G., Breil, M., Cozzi, G., Heinke, J., Jach, L., Niermann, D., Petrovic, D., Richling, A., Riebold, J., Steidl, S., Suarez-Gutierrez, L., Tradowsky, J. S., Coumou, D., Düsterhus, A., Ellsäßer, F., Fragkoulidis, G., Gliksman, D., Handorf, D., Haustein, K., Kornhuber, K., Kunstmann, H., Pinto, J. G., Warrach-Sagi, K., and Xoplaki, E.: The extremely hot and dry 2018 summer in central and northern Europe from a multi-faceted weather and climate perspective, Natural Hazards and Earth System Sciences, 23, 1699–1718, https://doi.org/10.5194/nhess-23-1699-2023, 2023.

Rubio-Martin, A., Pulido-Velazquez, M., Macian-Sorribes, H., and Garcia-Prats, A.: System dynamics modeling for supporting drought-oriented management of the jucar river system, Spain, Water (Switzerland), 12, https://doi.org/10.3390/w12051407, 2020.

Sacks, W. J., Cook, B. I., Buenning, N., Levis, S., and Helkowski, J. H.: Effects of global irrigation on the near-surface climate, Climate Dynamics, 33, 159–175, https://doi.org/10.1007/s00382-008-0445-z, 2009.

Shrestha, P. and Simmer, C.: Modeled land atmosphere coupling response to soil moisture changes with different generations of land surface models, Water (Switzerland), 12, https://doi.org/10.3390/w12010046, 2020.

https://doi.org/10.5194/egusphere-2026-3354
Preprint. Discussion started: 10 July 2026

Siebert, S., Henrich, V., Frenken, K., and Burke, J.: Update of the digital global map of irrigation areas to version 5., Tech. rep., Institute of Crop Science and Resource Conservation, Rheinische Friedrich-Wilhelms-Universität Bonn, https://doi.org/10.13140/2.1.2660.6728, 2013.

Taylor, K. E.: Truly conserving with conservative remapping methods, Geoscientific Model Development, 17, 415–430, https://doi.org/10.5194/gmd-17-415-2024, 2024.

Thiery, W., Davin, E. L., Lawrence, D. M., Hirsch, A. L., Hauser, M., and Seneviratne, S. I.: Present-day irrigation mitigates heat extremes, Journal of Geophysical Research, 122, 1403–1422, https://doi.org/10.1002/2016JD025740, 2017.

Thiery, W., Visser, A. J., Fischer, E. M., Hauser, M., Hirsch, A. L., Lawrence, D. M., Lejeune, Q., Davin, E. L., and Seneviratne, S. I.: Warming of hot extremes alleviated by expanding irrigation, Nature Communications, 11, https://doi.org/10.1038/s41467-019-14075-4, 2020.

Udina, M., Peinó, E., Polls, F., Mercader, J., Guerrero, I., Valmassoi, A., Paci, A., and Bech, J.: Irrigation impact on boundary layer and precipitation characteristics in Weather Research and Forecasting model simulations during LIAISE-2021, Quarterly Journal of the Royal Meteorological Society, https://doi.org/10.1002/qj.4756, 2024.

Valmassoi, A. and Keller, J. D.: A review on irrigation parameterizations in Earth system models, Frontiers in Water, 4, https://doi.org/10.3389/frwa.2022.906664, 2022.

Valmassoi, A., Dudhia, J., Sabatino, S. D., and Pilla, F.: Regional climate impacts of irrigation in northern Italy using a high resolution model, Atmosphere, 11, https://doi.org/10.3390/ATMOS11010072, 2020a.

Valmassoi, A., Dudhia, J., Sabatino, S. D., and Pilla, F.: Evaluation of three new surface irrigation parameterizations in the WRF-ARW v3.8.1 model: The Po Valley (Italy) case study, Geoscientific Model Development, 13, 3179–3201, https://doi.org/10.5194/gmd-13-3179-2020, 2020b.

Valmassoi, A., Keller, J. D., , Anlauf, H., Cress, A., Becker, A., Fundel, F., Hanisch, T., Kaspar, F., Krebber, Lange, M., Steinert, T., Wahl, S., Zängl, G., and Potthast, R.: ICON-DREAM – ICON Dual resolution Reanalysis for Emulators, Applications and Monitoring, https://doi.org/10.5676/dwd/icon-dream_v1, 2025.

Wenzel, J. L., Conrad, C., Piernicke, T., Spengler, D., and Pöhlitz, J.: Assessing the Impact of Different Irrigation Levels on Starch Potato Production, Agronomy, 12, https://doi.org/10.3390/agronomy12112685, 2022.

Wilks, D. S.: On "Field Significance" and the False Discovery Rate, Journal of Applied Meteorology and Climatology, 45, 1181 – 1189, https://doi.org/10.1175/JAM2404.1, 2006.

Wu, L., Feng, J., and Miao, W.: Simulating the Impacts of Irrigation and Dynamic Vegetation Over the North China Plain on Regional Climate, Journal of Geophysical Research: Atmospheres, 123, 8017–8034, https://doi.org/10.1029/2017JD027784, 2018.

Yang, Z., Qian, Y., Liu, Y., Berg, L. K., Hu, H., Dominguez, F., Yang, B., Feng, Z., Gustafson, W. I., Huang, M., and Tang, Q.: Irrigation Impact on Water and Energy Cycle During Dry Years Over the United States Using Convection-Permitting WRF and a Dynamical Recycling Model, Journal of Geophysical Research: Atmospheres, 124, 11 220–11 241, https://doi.org/10.1029/2019JD030524, 2019.

Yao, Y., Ducharne, A., Cook, B. I., Hertog, S. J. D., Aas, K. S., Arboleda-Obando, P. F., Buzan, J., Colin, J., Costantini, M., Decharme, B., Lawrence, D. M., Lawrence, P., Leung, L. R., Lo, M. H., Devaraju, N., Wieder, W. R., Wu, R. J., Zhou, T., Jägermeyr, J., McDermid, S., Pokhrel, Y., Elling, M., Hanasaki, N., Muñoz, P., Nazarenko, L. S., Otta, K., Satoh, Y., Yokohata, T., Jin, L., Wang, X., Mishra, V., Ghosh, S., and Thiery, W.: Impacts of irrigation expansion on moist-heat stress based on IRRMIP results, Nature Communications, 16, https://doi.org/10.1038/s41467-025-56356-1, 2025.

https://doi.org/10.5194/egusphere-2026-3354
Preprint. Discussion started: 10 July 2026

Zappa, L., Dari, J., Modanesi, S., Quast, R., Brocca, L., Lannoy, G. D., Massari, C., Quintana-Seguí, P., Barella-Ortiz, A., and Dorigo, W.: Benefits and pitfalls of irrigation timing and water amounts derived from satellite soil moisture, Agricultural Water Management, 295, https://doi.org/10.1016/j.agwat.2024.108773, 2024.

Zeng, Y., Xie, Z., and Liu, S.: Seasonal effects of irrigation on land–atmosphere latent heat, sensible heat, and carbon fluxes in semiarid basin, Earth System Dynamics, 8, 113–127, https://doi.org/10.5194/esd-8-113-2017, 2017.

Zhou, T., Leung, L. R., Leng, G., Voisin, N., Li, H. Y., Craig, A. P., Tesfa, T., and Mao, Y.: Global Irrigation Characteristics and Effects Simulated by Fully Coupled Land Surface, River, and Water Management Models in E3SM, Journal of Advances in Modeling Earth Systems, 12, https://doi.org/10.1029/2020MS002069, 2020.

Zhu, W., Baumert, J., Storm, H., Heckelei, T., and Siebert, S.: ECIRA - European crop-specific irrigated area at 1 km resolution annually from 2010 to 2020, Scientific Data, 12, 1349, https://doi.org/10.1038/s41597-025-05628-y, 2025.